BACHELOR THESIS

ACTUATION OF IRONSPERM WITH A ROTATING MAGNETIC FIELD

Vera Leeman

ENGINEEERING TECHNOLOGY - BIOMECHANICAL ENGINEERING

EXAMINATION COMMITTEE
prof.dr. S. Misra
prof.dr.ir. L. Abelmann
dr. I.S.M. Khalil

DOCUMENT NUMBER
BE - 876

UNIVERSITY OF TWENTE.

07 2022

Abstract

IRONSperm are dead bovine sperm cells that are coated with ferromagnetic iron-oxide particles. This coating provides a magnetic moment to the sperm cells, which makes them able to swim under the influence of an external magnetic field. IRONSperm are promising for targeted drug delivery, because their swimming direction can be controlled by the direction of the magnetic field. This research aims to provide an understanding in the swimming mechanisms of IRONSperm, by providing the mathematical principles of flagellar propulsion and experimental data on the swimming pattern of IRONSperm.

IRONSperm has been fabricated with electrostatic self-assembly of rice-shaped iron-oxide particles with the sperm cells.As a result of magnetic torque, the IRONSperm samples rotates along their long axis. The rotation of the flagellum generates a propulsive thrust from the flagellum in accordance with resistive force theory, which makes the IRONSperm swim perpendicular to the rotating magnetic field. The flagellar wave of IRONSperm is independent of the actuation frequency which is evidence of IRONSperm being a rigid swimmer. The swimming speed of IRONSperm is independent of the field strength of the external magnetic field. Increasing the frequency of the field, increased swimming speed for frequencies below the step-out frequency. The swimming speeds showed a significant drop once the step-out frequency was exceeded.

Contents

1 Introduction

1.1 Microrobotics

Microrobotics is an emerging part of research in the field of biomedical engineering [1]. It is particularly of interest because of its many possible applications. Microrobots can be useful for medical applications such as targeted drug delivery, sensing, and taking biopts.
With the help of microrobotics, procedures can become less invasive, which benefits the patients by reducing recovery time and risks. Targeted drug delivery is one of the main applications of clinical microrobotics [2]. The small size of microrobots allows them to reach many parts in the human body using the bodily systems. Here they can precisely drop off medication. Targeting exact locations for delivery minimizes side effects, decreases drug-intake frequency, increases the effectiveness and improves in vivo drug stability.

One case in which targeted drug delivery would greatly benefit the patient would be breast cancer. Breast cancer is the most common form of cancer for women and annually causes more than 40000 deaths [3]. Breast cancer is currently often treated with chemotherapy [4], which also targets healthy cells and tissue. Targeted drug delivery would allow for lower drug dosage and less targeting on nearby healthy tissue. This would greatly decrease side effects resulting of the treatment and improve the quality of life of the patient.

1.2 IRONSperm

IRONSperm is a bio-hybrid microrobot that might be able to perform targeted drug delivery [5]. IRONSperm are fabricated by electrostatically surrounding bovine sperm cells with ferromagnetic nanoparticles. The magnetic particles provide magnetic moment to the sperm cells which makes them actuatable using magnetic fields. The direction of IRONSperm will be controlled by the rotation axis of the magnetic field. Because of their swimming abilities, IRONSperm are very interesting as drug carriers.

Using bovine sperm cells instead of artificially created microrobots has the advantage that the optimal geometry of sperm cells and their organic bodies is preserved. The first assures optimal locomotion, while the latter provides an organic host for drug delivery. This is favourable because it assures biodegradability. Furthermore, the immune response to bio-hybrid robots will likely be minor, although research still has to be done on this. IRONSperm is discussed in greater detail in section 2.

1.3 Research Goal

As explained in 1.2, IRONSperm is a very promising tool for targeted drug delivery. To use IRONSperm in clinical applications, it is important that the way of movement is fully understood, so the conditions of the applied magnetic field can be optimized to maximize the swimming speed. This research aims to provide an understanding of the behaviour of IRONSperm when exposed to a rotating magnetic field, so that its behaviour in future clinical applications can be understood and optimized.

1.4 Research question

The main question that this research will try to answer will be:

How does IRONSperm behave when exposed to a rotating magnetic field?

To answer this question, other questions will have to be answered in the process. These are:

- How does flagellar movement generate propulsion?
- What are the effects of different fabrication methods?
- How can the flexibility of the flagellum be characterized?
- How does IRONSperm orient itself with respect to the magnetic field?
- What are the effects of the frequency and field strength on the swimming speed of IRONSperm?

1.5 Hypothesis

It is hypothesized that IRONSperm will react to a magnetic field because of the magnetic torque that results from the magnetization factor in the samples and the rotating magnetic field. It is expected that IRONSperm aligns itself perpendicular to the rotating magnetic field. Due to the rotating magnetic field, IRONSperm will rotate with it and this will induce a propagating wave in the tail. The wave propagation will generate a thrust that propels the IRONSperm forward. The magnitude of this thrust will be according to the resistive force theory.

The fabrication method of IRONSperm is based on electrostatic self-assembly. It is expected that this fabrication method results in a large cell-to-cell variability between the samples because this method of fabrication is based on the surface charge. The surface charge is variable from cell to cell. It is expected that a larger coverage results in a better response to the magnetic field because the magnetic torque is larger. This will experimentally show as a larger swimming speed and better alignment.

It is expected that coating the samples with rice grain-shaped feromagnetic nanoparticles will lead to the IRONSperm with the largest magnetic moment. Selecting the sperm with the largest swim-up time before electrostatic self-assembly is performed is hypothesized to increase the amount of bundling in the sample. In the case that spinell particles are used instead of rice grain-shaped maghemite, it is expected that nanoparticles will mainly adhere to the head. Therefore, it is hypothesized that a coating with spinell particles yields IRONSperm that are bundled at the head.

A minimal magnetic torque is needed to overcome the drag torques acting on the sperm cell. The hypothesis is that larger field strengths increase the torque and therefore allow for rotation of the IRONSperm. Increasing the field strength when the sperm-cell is already rotating with the field, will not have an effect on the swimming speed, as the IRONSperm will not be able to rotate faster than the external magnetic field. Increasing the frequency will likely increase the swimming speed, up to the step-out frequency. At this step-out frequency, the IRONSperm is no longer able to keep up with the rotating field and therefore will start a jerky motion instead of a continuous rotation. This will result in a decrease in propulsive thrust and therefore a vast decrease in swimming speed. Earlier research on IRONSperm have found this step-out frequency to be 8 Hz [5] and that IRONsperm swims with average speeds of 6.8 $\mu m/$s. Velocities and step-out frequencies of similar magnitude are expected in this research.

2 Properties of IRONSperm

2.1 Fabrication

The fabrication of IRONSperm is based on electrostatic self-assembly between bovine sperm cells and magnetic nanoparticles. IRONSperm is fabricated using rice grain-shaped ferromagnetic iron oxide particles and bovine sperm cells that are approximately 60 μm long. The magnetic nanoparticles are subjected to electrostatic forces [5]. Van der Waals forces, which increase as the distance between 2 particles decreases, cause the particles to aggregate. These aggregates are positively charged. The sperm cells have a net negative surface charge [6] and are therefore oppositely charged from the particle aggregates. Due to Coulomb forces, that exist in between two oppositely charged particles, the magnetic nanoparticles are attracted to the surface of the sperm-cells.

The distribution of particles along the surface of the sperm-cell is non-uniform. This is a result of the non-uniform charge along the surface of a sperm-cell [6] [7]. Even though the net surface charge is negative, some surface areas of the cell are positively charged. This means that electrostatic adhesion of the magnetic particles does not happen uniformly about the length of the sperm cell. Previous research [6] has shown that both positively and negatively charged particles attach to the surface of the sperm cell. The head of a sperm cell has a slightly positive charge, since it allows the binding of negatively charged particles. Negatively charged particles rarely bind on the flagellum, which suggests that the flagella are predominantly negatively charged.

The distribution of nanoparticles varies a lot due to the cell-to-cell variability in surface charge [6]. The charge distribution of a sperm cell depends on its developmental state [5]. Therefore it is expected that there is a large sample variance. Sperm cells that have a relatively negatively charge will attract more nanoparticles and will therefore experience a larger magnetic torque. Furthermore, the distribution of charges along the cell also differs from cell to cell. Therefore, the response to the applied magnetic field will change. In experiments, cell-to-cell variation will be observable as a large deviation of velocities and step-out frequencies between different IRONSperm.

The net charge and spatial distribution along the sperm cell are important factors in the determination of the magnetization profile. The goal is to fabricate samples with high magnetization, such that IRONSperm will respond to magnetic fields in the millitesla range but to also keep the flagellum flexible to allow flagellar wave propagation. Increasing the amount of magnetic particles results in a higher magnetization but it also decreases the flexibility of the flagellum. To allow for a traveling wave in the tail, it is necessary to have a flexible flagellum and therefore an optimum for the amount of particles exists.

2.1.1 Fabrication of multi-flagellar IRONSperm

In addition to the research to single-flagellar IRONSperm, it has also been of interest to study IRONSperm with multiple flagella. IRONSperm with multiple flagella can be obtained by bundling multiple IRONSperm at the head. This will result in a sample that looks like it has one head and multiple tails. In attempt to fabricate multi-flagellar IRONSperm the same general approach has been taken although some changes have been made to the process. Two fabrication methods have been tested out to promote bundle formation.

The first approach has been to promote bundle formation before adding iron-oxide particles. First a swim-up of sperm is performed to seperate the most motile spermcells from the rest. This increases the post-thawing swimming time. It has been observed that the amount of bundling increases with an increased swimming time. Therefore, performing a swim-up yields samples with a relatively high chance of bundle formation. After the swim-up, the samples are washed with distilled water and incubated with rice-shaped magnetic iron oxide particles, where the particles adhere to the sperm cells by electrostatic self-assembly as described above.

The second fabrication method uses spinell iron oxide particles instead of rice shaped particles. These particles have a positive charge which is opposite from the rice shaped particles because they have been coated with silicon oxide. As mentioned before, although the sperm cell has a net negative surface charge, some areas on the surface have a positive charge. Therefore, the negatively charged spinell particles will still be able to bind to the sperm cell by electrostatic self-assembly. Since the head of the sperm cell has a net positive charge, negatively charged particles mainly bind to the head. Therefore, the spinell particles will attach mostly to the head. Multi-flagellar IRONSperm are a result of bundling at the head. Attaching the magnetic particles mainly to the head of the sperm, is hypothesized to promote bundling at the head which could lead to multi-flagellar IRONSperm.

2.2 Magnetic characterization of IRONSperm

2.2.1 Estimation of magnetic moment

To obtain a value for the magnetic torque that is exerted on the IRONSperm, a value for the magnetic moment is necessary. This magnetic moment depends on the volume and magnetization value. To estimate the magnetic moment for IRONSperm, the magnetic moment of the iron-oxide particles should be found and this should be multiplied by the amount of particles. The magnetic moment can also be determined by a theoretical model that is described in B.

Earlier research [5] that studied IRONSperm has measured the magnetic moment of IRONSperm with a vibrating sample magnetometer on a sample with a known concentration of IRONSperm. They found that the average magnetic dipole moment $5.9 \times 10^{-11} Am^2$. Although these samples are likely not exactly the same, this value can be used to formulate an expectation. The actual experimental observations may differ a lot due to cell-to-cell variability and because the magnetic moment is not calculated for these specific samples. These calculations however, allow for an estimation and therefore can be used to compare with the experimental results.

2.2.2 Magnetic segmentation

As explained in the fabrication section 2.1, the process used to bind particles to the sperm cells is electrostatic self assembly. This introduces a large variability in the locations of the particles on the flagellum. These particles will then also respond to the magnetic field and have a resulting magnetic torque. As a result of the change in distribution of the bending moment, the waveform is altered [8]. This will have an effect on the propulsive thrust which results in an effect on the velocity.

Earlier research into the effect of segmented magnetization on flagellar propulsion [8] has shown a great variation of produced thrust between different configurations of IRONSperm. It has been found that the maximum thrust is obtained when the head, principal piece and distal ends of the sperm cell are magnetized.

In case the flagellum is rigid, the waveform is constant and therefore the distribution of the particles will not have as much of an effect on the swimming speed of the particles. However, the distribution of the particles might be related to the shape of the rigid flagellum.

2.3 Differences between IRONSperm and motile sperm cells

Although IRONSperm is fabricated from natural sperm cells, they do not exhibit the same propulsion mechanisms. Therefore, models of the propagation of natural sperm cells are only partially applicable to this research. The most important difference in analyzing propulsion mechanisms for sperm cells in contrast to IRONSperm is that motile sperm cells also actuate themselves from the tail in addition to actuation from the head. Natural sperm cells therefore produce flow fields with gradually increasing velocity toward the free distal end of the flagellum [8]. In contrast to motile spermcells, IRONSperm has a passive flagellum.

Because of the actively actuated flagellum, motile spermcells show a different waveform than magnetically actuated sperm. The waveform is directly related to the thrust that is produced according to resistive force theory, which is explained in detail in section 3. In addition to the lower propulsive thrust, the drag force on IRONSperm is also higher as a result of the iron-oxide particles. Earlier research on the differences between motile sperm cells and IRONSperm [9] has found the average path velocities to be 113.2 μm/s for motile sperm cells and 7.3 μm/s for IRONSperm.

3 Movement of IRONSperm

To propel through the medium, IRONSperm must produce a force that is larger than the drag force acting in the direction opposite to the movement. This propulsive force is produced by the flagellar movement.Due to the very small size of IRONSperm, it does not swim using impulse but rather creates thrust as a result of a drag anisotropy. In this section, resistive force theory is discussed to explain the propulsion of IRONSperm.

3.1 Wave propagation along a flagellum

Assuming that IRONSperm flagella are rigid, both natural sperm cells and IRONSperm move as a result of wave propagation along the flagellum. To obtain wave propagation in the flagellum, the IRONSperm is rotated along its long axis. Therefore there is a motion in the head, and the flexible tail that trails behind starts forming waves. Two forces govern the movement of the flagella [10] [11] [12]; (1) The elastic forces that try to straighten the flagellum back to its original shape and (2) Viscous forces that result from the medium and oppose the motion. These forces can be seen in figure 1.

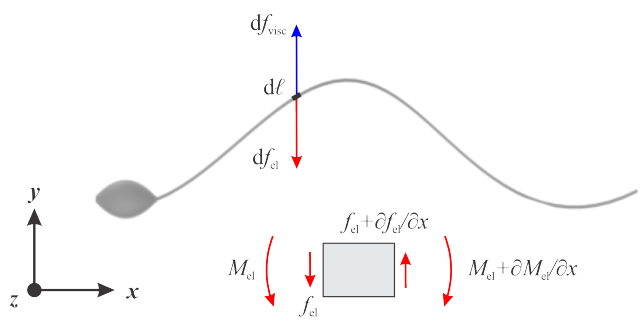

Figure 1: Force balance consisting of the viscous forces (df_{visc}) and the elastic forces (df_{el})acting on a small element dl of a flagellum. The elastic forces try to straighten the flagellum back to its natural shape while the viscous forces oppose this motion. [11]

To model the forces acting on the flagellum, a small element dl is chosen. The elastic force acting on the element is:

$$df_{el} = -ESK^2 \frac{\partial^4 y}{\partial x^4} dl \tag{1}$$

Here, E is the Young's modulus, K is the radius of gyration of the section and S is the cross-sectional area. x and y are defined as the coordinate system in figure 1.

The viscous forces acting on the element can be derived from the formula for the drag of a cylinder at low Reynolds numbers.

$$dF_V = \frac{4\pi\mu}{2.0 - \log(Re)} \frac{\partial y}{\partial t} dl \tag{2}$$

In this equation, μ is the drag coefficient, y is the displacement in vertical direction, and t is the time. Re is the Reynolds number which is defined as:

$$Re = \frac{\rho v l}{\mu} \tag{3}$$

Where in this equation, ρ is the density of the fluid, v is the fluid velocity, l is the length of the IRONSperm, and μ is again the viscosity.

Equation 2 is an approximation of reality and is only valid for low Reynolds number. Since IRONSperm is very small, the Reynolds number in this situation is also very small. Therefore, these approximations hold.
Equation 2 is strictly not linear, since the Reynolds number is also dependent on $\frac{\partial y}{\partial t}$. However, since the change is very small in this situation, the dependency can be neglected.
Furthermore, it stands out that the logarithm of the Reynolds number should not equal 2, because that will result in a division by 0. For IRONSperm in water, the Reynolds number will be in the order of 1×10^{-3} to 1×10^{-5}, therefore there will be no division by zero in this case.

The governing equation for the motion can be found by setting up a balance between these two forces:

$$\begin{aligned} -ESK^2 \frac{\partial^4 y}{\partial x^4} dl &= \frac{4\pi\mu}{2.0 - \log(Re)} \frac{\partial y}{\partial t} dl \\ \frac{\partial^4 y}{\partial x^4} &= -\frac{1}{ESK^2} \frac{4\pi\mu}{2.0 - log(Re)} \frac{\partial y}{\partial t} \end{aligned} \tag{4}$$

A steady state solution to this equation can be found. For this solution the following boundary conditions have been applied: The boundary conditions that are applicable to the system of IRONSperm with a single flagellum are:

$$\begin{aligned} y &= 0 \text{ at } x = 0 \text{ for all t} \\ \frac{\partial y}{\partial x} &= Ge^{i2\pi ft} \text{at } x = 0 \\ \frac{\partial^2 y}{\partial x^2} &= 0 \text{ at the distal end} \\ \frac{\partial^3 y}{\partial x^3} &= 0 \text{ at the distal end} \end{aligned}$$

The first and second boundary condition are the result of the flagellum being attached to a stationary head, which

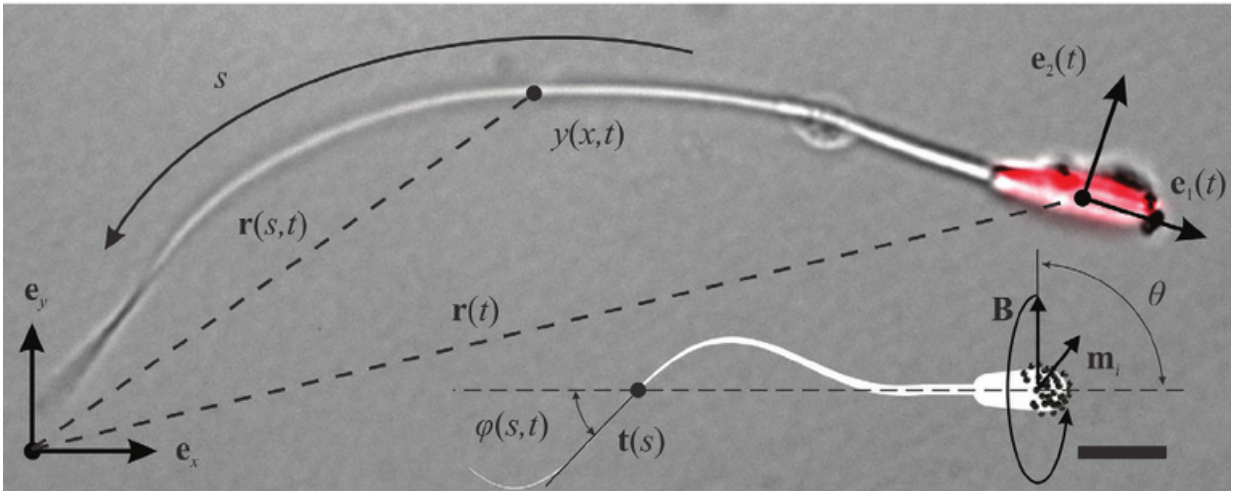

Figure 2: This figure shows the parameters that are used to describe flagellar beat pattern. The flagellum has an arc length s. The local coordinate system e(t) is centered at the head. The position vector is dependent on space and time and is given by r(s,t). r(t) is the position of the center of the sperm head [8].

can be modelled as a system that is constrained to move about a rigid hinge. In the second boundary condition, G is the amplitude of the wave. The boundaries at the distal end arise from the fact that both the bending moment $\frac{\partial^2 y}{\partial x^2}$ and the shear forces $\frac{\partial^3 y}{\partial x^3}$ become zero at the distal end where the element is free.

Finding a steady state solution for this equation characterizes the flagellar beat pattern [8] [13]. Using the boundary conditions, the flagellar beat pattern can be described as:

$$\mathrm{r(s,t) = r(t) - ae_1(t) - \int_0^s \cos\phi(s,t)e_1(t) + \sin\phi(s,t)e_2(t)dv} \tag{5}$$

The parameters are defined as in figure 2. A frame of reference $(e_1(t), e_2(t))$ is used. As depicted in figure 2 this frame of reference is centered at the head. r(s,t) is the position vector of the flagellum centerline to the frame of reference. r(t) is the position of the center of the sperm head and 2a is the major diameter of the sperm head.

$\phi(s,t)$ is the time and space dependent tangent angle between the flagellum and the centerline. The tangent angle can be described by taking its zeroth (ϕ_0) and first (ϕ_1) Fourier mode. Higher Fourier modes do not need to be taken into account because they contribute very little (<5%) to the tangent angle.

$$\phi(\mathrm{s,t}) = \phi_0(\mathrm{s}) + \phi_1(\mathrm{s})\mathrm{e}^{\mathrm{i}\omega\mathrm{t}} + \phi_1^*(\mathrm{s})\mathrm{e}^{-\mathrm{i}\omega\mathrm{t}} \tag{6}$$

From this equation, the wave variables can be obtained. The mean flagellar curvature (K_0) is characterized by the zeroth mode as $\phi_0 = K_0 s$. The bending amplitude (A_0) is characterized by the first mode as $|\phi_1| = A_0 s$. The wave propagation speed ($\omega = \frac{2\pi}{\lambda}$) is characterized by $arg(\phi_1)$.

Therefore the tangent angle can be rewritten as [14]:

$$\phi(s,t) = K_0 s + 2A_0 s cos(\omega t - \frac{2\pi s}{\lambda}) \tag{7}$$

3.2 Drag based thrust

To actually propel forward, a so-called drag based thrust has to be created by the flagellum. To do this, the velocities and forces in the tail are split up in parallel and perpendicular components as can be seen in figure 3. The velocity is defined as the first time derivative of the position vector.

From figure 3 it follows that

$$\mathrm{U}_\perp = \mathrm{U}\sin(\theta) \tag{8}$$

$$\mathrm{U}_\parallel = \mathrm{U}\cos(\theta) \tag{9}$$

where U is the velocity and θ is the angle between the element dl and u.

The flagella pushes to its surroundings with a drag force $\mathrm{f}_\perp$ in the normal direction and $\mathrm{f}_\parallel$ in tangential direction. For the small element dl, the forces can be found by:

$$\mathrm{df}_\perp = -\xi_\perp \mathrm{U}_\perp \mathrm{dl} \tag{10}$$

$$\mathrm{df}_\parallel = -\xi_\parallel \mathrm{U}_\parallel \mathrm{dl} \tag{11}$$

Here $\xi_\perp$ and $\xi_\parallel$ are the drag coefficients in the normal and tangential direction respectively. The net force that is exerted by element dl in the x direction can be found by adding the components of the working in the x direction. As can be seen in figure 3 this leads to the equation:

$$\mathrm{df} = \mathrm{df}_\parallel \sin(\theta) - \mathrm{df}_\perp \cos(\theta) \tag{12}$$

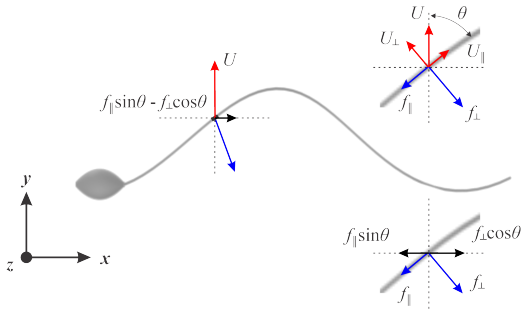

Figure 3: The velocity, u, with which a small element dl is moving, is resolved into a normal $u_{\parallel}$ and a tangential $u_{\perp}$ component. The force that the element delivers is also split up in a normal and tangential component. The angle between the element dl and the direction of the velocity u is defined as θ. [11]

Equation 12 can be filled in with the expressions found in 10 and 11. Thereby the following expression is obtained:

$$\begin{aligned} \mathrm{df} &= \mathrm{df}_{\parallel}\sin(\theta) - \mathrm{df}_{\perp}\cos(\theta) \\ &= (\xi_{\perp}\mathrm{U}_{\perp}\cos(\theta) - \xi_{\parallel}\mathrm{U}_{\parallel}\sin(\theta))\mathrm{dl} \\ &= (\xi_{\perp}\mathrm{U}\sin(\theta)\cos(\theta) - \xi_{\parallel}\mathrm{U}\cos(\theta)\sin(\theta))\mathrm{dl} \\ &= (\xi_{\perp} - \xi_{\parallel})\mathrm{U}\sin(\theta)\cos(\theta)\mathrm{dl} \end{aligned} \tag{13}$$

From this equation it follows that there is a net propulsive force generated if $\xi_{\perp} \neq \xi_{\parallel}$ This means that there is only a propulsive force if there is drag anisotropy. The drag anisotropy is a result of having a long and slender element such as a flagellum. Drag anisotropy is explained in more detail in section A of the appendix.

For a propagating wave along a flagellum, the generated propulsive force can be found with equation 14

$$f = (\xi_{\perp} - \xi_{\parallel}) \int_0^L \frac{\partial y}{\partial t}\frac{\partial y}{\partial x}\, dx \tag{14}$$

This equation gives the propulsive force for a specific time-dependent deformation of the flagellum. In this research, the filament will be periodically oscillating and therefore, the force must be averaged over one period of oscillation.

$$\langle f \rangle = (\xi_{\perp} - \xi_{\parallel}) \langle \int_0^L \frac{\partial y}{\partial t}\frac{\partial y}{\partial x}\, dx \rangle \tag{15}$$

3.3 Planar vs helical motion

There are two modes of propulsion with which IRONSperm can move; planar and helical flagellar motion. Planar flagellar motion can be induced by an oscillatory magnetic field, which results in an oscillatory movement of the head. Due to the flexibility of the flagellum, this also induces an oscillatory movement in the flagellum which causes propulsion. Helical flagellar motion can be induced by a rotating magnetic field, which causes the head to rotate. This induces a helical shape in the flagellum. In natural eukaryotic sperm cells, switching between these two ways of movement has been observed as a result of altering viscocity [15]. In the case of IRONSperm, switching can be achieved by changing the magnetic field [16] from rotating to oscillating.

For both modes of movement, the propulsive force is generated using drag based thrust as described above. In earlier research on single-flagellar IRONSperm [16] it has been found that helical flagellar propulsion is more efficient than planar propulsion for relatively low actuation frequencies (<6Hz). This is because the time dependent deformation of the flagellum is larger when rotating the flagellum, and according to equation 15 this leads to a larger propulsive thrust. As the flagellar amplitude decreases when rotating a flexible flagellum with high frequencies, the deformation decreases and less thrust is generated. Planar propulsion might prove to be more useful at high actuation frequencies.

In this research only relatively low frequencies <3Hz have been researched. Therefore, only helical motion was studied.

4 Magnetic actuation

To actuate the magnetized sperm cells, an external rotating magnetic field is applied [5]. This way of actuation has been used in many other types of microrobots, and has been proven succesful in multiple cases [1]. The ferromagnetic particles in the IRONSperm try to orient themselves in such a way that they are aligned to the magnetic field. Therefore, applying the magnetic field leads to a magnetic torque in in the IRONSperm. As a result of this torque, IRONSperm starts rotating and creates a travelling wave from the head to the distal end in the flagellum. An important condition for this to occur, is that the flagellum is flexible, since a traveling wave can not occur in a rigid body. In case of a rigid flagellum, no wave is created, but the IRONSperm simply starts rotating around its long axis. If the flagellum is curved, this will also result in drag based thrust as described in section 3.2.
If the external magnetic field is rotating, the feromagnetic particles will be constantly misaligned. Therefore, a rotating magnetic field will results in a continuous magnetic torque and therefore the IRONSperm will rotate

4.1 Helmholtz coils

To apply the external magnetic field, Helmholtz coils are used. A Helmholtz coil pair [17] consists of two identical circular coils aligned on the same axis, that are separated by a distance that is equal to the radius of the coil, through which an identical current runs in the same direction. This can be used to generate an uniform magnetic field. To create a rotating magnetic field, three coil pairs have to be placed orthogonally to create a 3D Helmhotlz configuration. This configuration is preferred because it generates only pure magnetic torque with negligible applied magnetic forces[18].

The rotating magnetic field that is created by the 3D Helmholtz configuration can be described by equation 16 [19].

$$\overrightarrow{B}(\mathrm{t}) = \mathrm{B}_0 \begin{bmatrix} cos(\omega_m t) \\ sin(\omega_m t) \\ 0 \end{bmatrix} \tag{16}$$

In this equation B_0 is the magnitude of the magnetic field. For this research B_0 will be in the millitesla range. ω_m is the magnetic rotation rate. ω_m is related to the field frequency (f_m) with equation 17

$$\omega_\mathrm{m} = 2\pi \mathrm{f}_\mathrm{m} \tag{17}$$

Equation 16 is valid for a field that rotates around the z axis. Therefore, the field strength acting in the z direction equals 0. Since IRONSperm moves in the direction perpendicular to the rotating field, it would be swimming along the z-axis for this situation.

4.2 Magnetic torque and force

The Helmholtz configuration produces a magnetic field which exerts a magnetic force and a magnetic torque on the IRONSperm.

The magnetic force [20] can be found with:

$$\overrightarrow{F_M} = (\overrightarrow{m} \cdot \nabla)\overrightarrow{B} \tag{18}$$

The magnetic moment [21] that is exerted on the IRONSperm can be found with:

$$\overrightarrow{T_M} = \overrightarrow{m} \times \overrightarrow{B} \tag{19}$$

In both equations, B is the magnetic induction of the field which follows from equation 16 and m is the magnetic moment of the IRONSperm. The magnetic moment of a particle is dependent on its volume (v) and magnetization (M) according to equation 20

$$\overrightarrow{m} = \overrightarrow{M} \times \overrightarrow{v} \tag{20}$$

To rotate IRONSperm, the magnetic torque supplied from the external field must be equal to the viscous torque [22]. At low Reynolds numbers, which apply to this situation, the external nonfluidic (magnetic) force and torque are linearly related to its linear and rotational velocities by a symmetric matrix according to equation B.16 [23, 1].

$$\begin{bmatrix} \overrightarrow{F_m} \\ \\ \overrightarrow{T_m} \end{bmatrix} = \begin{bmatrix} \mathrm{a} & \mathrm{b} \\ \mathrm{b} & \mathrm{c} \end{bmatrix} \begin{bmatrix} \overrightarrow{v} \\ \overrightarrow{\omega} \end{bmatrix} \tag{21}$$

Here F_m and T_m are defined according to equations 18 and 19. V is the linear velocity and ω is the rotational velocity. The coefficients of the drag matrix are experimentally determined for the case where a flagellum is rigidly attached to a body [24]. They depend on the viscosity of the fluid and the geometrical properties of the swimmer [23, 24]. The definition of these values can be found in appendix B.

4.3 Effect of field parameters

To study the behaviour of IRONSperm in a magnetic field, both the field strength and the frequency of the field generated by the Helmholtz coils will be experimentally altered.

4.3.1 Field strength

An increase in the field strength (B_0) is directly related to an increase the magnetic torque according to equation 19. An increase in torque will lead to an increase in both rotational and translational velocity according to equation B.16. However, the torque is dependent on the angle between the magnetic moment and the magnetic field.

Therefore, the torque will decrease as the distance between the magnetic moment and magnetic field vectors decreases. This means that an IRONSperm will not be able to rotate with a frequency that is larger than the actuation frequency. An increase in field-strength will thus not necessarily lead to an increase in torque, and therefore it is expected that increasing the field strength does not show an increase in swimming velocity.

4.3.2 Frequency

It is expected that increasing the frequency of the external magnetic field will lead to an increase in swimming speed. . Increasing the rotational frequency of the IRONSperm will cause a larger deformation in a certain time, and therefore according to resistive force theory and equation 15 will lead to a larger propulsive thrust and thus a higher swimming velocity.
This expectation can also be derived from B.16. In this research, it is reasonable to assume that the magnetic force is 0. This is a reasonable assumption because due the field is rotating and therefore, the pulling force goes to 0 [23]. If it is assumed that the magnetic force is zero, equation B.16 can be rewritten into the following equation:

$$\mathrm{F_m} = \mathrm{a} * \mathrm{v} + \mathrm{b} * \omega = 0 \tag{22}$$

$$\mathrm{v} = -\frac{\mathrm{b}}{\mathrm{a}} * \omega \tag{23}$$

$$\mathrm{v} = -\frac{\mathrm{b}}{\mathrm{a}} * 2\pi \mathrm{f} \tag{24}$$

This shows that there is a linear relation between the frequency and the velocity. Increasing the frequency will lead to an increase in v. The negative sign denotes the swimming direction. This linear relationship is also in accordance with earlier experimental data [25]. It should be noted that equation B.16 is derived for rigid microrobots. Due to the fact that the flagellar amplitude decreases at high frequencies for flexible tails, it is likely that the relationship between frequency and translational velocity is not perfectly linear for flexible IRONSperm.

4.3.3 Step-out frequency

As long as the applied magnetic field rotates sufficiently slowly, IRONSperm will synchronously rotate with the field. At a certain frequency, the applied magnetic torque is no longer strong enough to keep the microrobot synchronized with the field. This frequency is known as the step-out frequency. It has been shown that the velocity of microrobots drastically decreases above the step-out frequency [26].

The step-out frequency is dependent on the magnetization factor, viscous forces and the field strength. It is reached when the drag torque, that increases with an increase in rotational velocity, exceeds the maximal applicable magnetic torque.

Equation B.16 can be rewritten to calculate the translational and rotational velocities as follows:

$$\begin{bmatrix} \mathrm{v} \\ \omega \end{bmatrix} = \begin{bmatrix} \mathrm{a} & \mathrm{b} \\ \mathrm{b} & \mathrm{c} \end{bmatrix}^{-1} \begin{bmatrix} \mathrm{F_m} \\ \mathrm{T_m} \end{bmatrix} \tag{25}$$

$$\begin{bmatrix} \mathrm{v} \\ \omega \end{bmatrix} = \frac{1}{\mathrm{ac} - \mathrm{b}^2} \begin{bmatrix} \mathrm{c} & -\mathrm{b} \\ -\mathrm{b} & \mathrm{a} \end{bmatrix} \begin{bmatrix} \mathrm{F_m} \\ \mathrm{T_m} \end{bmatrix} \tag{26}$$

From equation 26 the relationship between the rotational speed and the torque can be found.

$$\omega = -\frac{\mathrm{b}}{\mathrm{ac} - \mathrm{b}^2}\mathrm{F_m} + \frac{\mathrm{a}}{\mathrm{ac} - \mathrm{b}^2}\mathrm{T_m} \tag{27}$$

Since the force is assumed to be zero. Equation 27 can be rewritten to be only dependent of T. Furthermore, it is known that $\omega = 2\pi f$. The equation for the step-out frequency then becomes:

$$\mathrm{f_{SO}} = \frac{1}{2\pi}\frac{\mathrm{a}}{\mathrm{ac} - \mathrm{b}^2}\mathrm{T_{max}} \tag{28}$$

The step out frequency is thus dependent on the drag coefficients. These are dependent on the viscosity and geometric parameters of the cell. The maximum torque that is available is dependent on the magnetization. Because a large variability of magnetization factors is expected, it is also expected that there is a large variability of step-out frequencies.

The step-out frequency also depends on the field strength. An increase in field strength is related to an increase in the maximum applied torque. Therefore it is expected that the step-out frequency is higher when the field strength is increased.

5 Method

5.1 Setup

To conduct measurements on the IRONSperm, an Helmholtz configuration in combination with a light microscope has been used. The Helmholtz consists of 3 pairs of coils that produce an homogeneous magnetic field. Using software to control the current that flows through the coils, a homogeneous rotating magnetic field can be obtained.
Measurements have been taken with lenses of a magnification factor of 20x and 10x. The objective and the camera add an extra magnification factor. To calculate the exact magnification of the gathered images, a microchip with a ruler has been used. This microchip can be seen in figure 4.

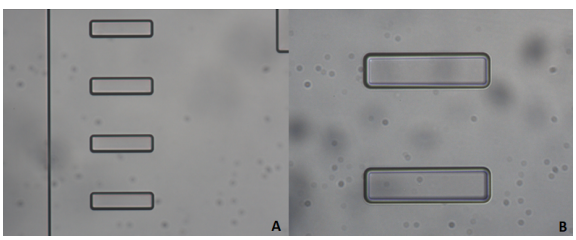

Figure 4: The microchip that is used to determine the measurements of the images. A) The ruler as seen with the 10x lens. B) The ruler seen with the 20x magnification. The distance between 2 ticks corresponds with 0.1 mm

The ruler has been measured to obtain a conversion rate between the images and the real dimensions. It has been found that for the 20x lens, the distance between 2 lines of the ruler corresponds with 8.8 centimeters in the pictures. For the 10x lens, 0.1 millimeter is measured to be 4.4 cm in the images. Therefore the total magnification of the setup is 880 times when using the 20x lens and 440x when using the 10x lens.
Since some measurements are taken in pixels a conversion factor to convert pixels to mm has also been calculated. The height of the image is 1032 pixels which corresponds with 18.2 centimeter. Therefore, $1px = \frac{18.2}{1032}$ centimeter. Since the magnification factor is known. It can be calculated that for the 20x lens:

$$\begin{aligned} 1\text{px} &= \frac{18.2}{1032} * \frac{1 \times 10^{-4}}{8.8} \\ &= 2.00 \times 10^{-7}\text{meter} \end{aligned} \tag{29}$$

For the 10x lens, the magnification is divided by two. Therefore, for 10x; 1px $= 1.00 \times 10^{-7}$ meter.

5.2 Samples

In this research IRONSperm samples that have been fabricated as described in 2.1 are used. They have been stored in the fridge to prevent agglomeration as much as possible. Before analysis, the samples were vortexed to obtain an homogeneous mixture for 30 seconds.

An 50% dilution was made by adding distilled water. This was done to reduce the amount of cells and other clutter in the volume, so that there was more space to swim for the IRONSperm. This dilution was also vortexed for 30 seconds to obtain an homogeneous mixture. Then 10 μl was pipetted to be observed under the microscope. For the observation, 2 different type of techniques were used.

In the first technique the droplet placed in a container, and slid directly under the microscope. This container is a glass microscope on which a hollow square of rubber material is placed. In this square, the droplet is placed.

The second technique that was suggested was the hanging droplet. The hanging droplet is a technique that is often used in the field of microbiology to observe samples. It is of interest to IRONSperm research because it was hypothesised that it would prevent the samples from getting stuck at the bottom of the container. This is one of the effects that has been observed in early experiments. IRONSperm would sink to the bottom of the container and get stuck. Here the adhesion forces would be larger than the produced thrust force. Therefore, samples would still react to the magnetic field, as they did produce a motion at the application of the magnetic field, but they are not able to propel themselves. The hanging droplet is obtained by pipetting a droplet on a microscope glass. This microscope glass is then quickly turned around and placed on a rubber ring that is placed on a microscope slide. This results in a droplet that is hanging and therefore gravity directs the samples away from the glass.

5.3 Prove rotation

To study the behaviour of IRONSperm under the influence of a rotating magnetic field, it is important that its way of movement is understood. It is expected that applying an external rotating field will induce a rotational movement in the head of the IRONSperm. As the data will be analyzed as two-dimensional videos, it could be difficult to tell if the IRONSperm is actually rotating in three dimensions. Therefore it is important to obtain videos in which it is clear that the IRONSperm is rotating in 3D. This can be seen by a top-view of a swimming IRONSperm, or by an IRONSperm that has a distinct feature from which rotation can be seen. Finally,

attention should be paid to the head. The head will likely be the region where the distinction between oscillatory 2D motion and rotational 3D motion is the most clear. In case of rotation in 3D, the shape of the spermcell-head will change, as the camera stands from a different angle. In 2D oscillatory movement, the head will keep the same shape, and will show a different angle with respect to the attachment point of the flagellum.

Rotation can also be shown by a colour change in the flagellum during a beat cycle. If the flagellum is indeed rotating, the colour when the wave is pointing towards the observer will be different than when the point of the flagellum is pointing away from the observer. This is because the flagellum will move out of focus during a rotation. If the flagellum is moving only in plane, the colour of a point of the flagellum will not vary.

It is important to prove if the IRONSperm are indeed moving in three dimensions because its way of movement will have strong effects on its speed. An IRONSperm that is moving in plane will likely yield very different results. To prevent wrong interpretations of the data, first an analysis of the way of movement is conducted.

5.4 Prove flexibility

In the resistive force theory, it has been assumed that the flagellum of the sperm cell is flexible, and therefore its shape is subject to change. To prove if the IRONSperm are indeed flexible, the envelope of motion of the IRONSperm will be observed. It has been shown before [5] that a higher actuation frequency corresponds with a lower wave amplitude. Flexibility of the samples can be proved by comparing the maximum amplitude of the wave at different frequencies. If the flagellum is flexible, the wave amplitudes will change.

The wave amplitude will be measured at the point in the flagellum where the highest flagellar displacement is at its maximum. The amplitude is defined as the distance from the centerline, which is the straight line through the tip of the head and the attachment point of the flagellum and the sperm head. It will be measured for 3 beat cycles per frequency, to even out errors.

Flexibility will also be visible during actuation. A rigid flagellum will keep the exact same shape at all times, if a change of shape is visible, the flagellum will be flexible. Closely inspecting the videos will likely give results on the flexibility of the flagellum. Another way to qualitatively prove the flexibility, is to rotate the IRONSperm in plane. A flexible flagellum will probably change shape during its rotation, while a rigid IRONSperm will stay straight during the rotation.
Combining these different techniques will make it possible to draw conclusions on the flexibility of IRONSperm.

5.5 Orientation of IRONSperm with respect to the magnetic field

To see how IRONSperm orients itself with respect to the magnetic field. The axis around which the external magnetic field is rotating will change to study the effect on the swimming direction of the IRONSperm. This will be done while the IRONSperm is swimming to see how well the IRONSperm can be steered.

In addition, there will also be an experiment were the field is not rotating. Instead there will then be a homogeneous magnetic field. The direction of the field will then be turned by 45 degrees (in plane). This will allow for measurements on how long it takes for the IRONSperm to turn towards the field.

5.6 Movement of the fluid

The fluid is moving due to a number of reasons. First there are the effects that are a direct result of experimental limitations. Since the scale the experiments are done on are very small, small disturbances to the setup will be very visible in the measurements. For instance, if someone is using the same table as the Helmholtz configuration, it could very well be that they bump into the table causing the droplet of IRONSperm to move. This will then cause a visible disturbance in the video analysis. These disturbances will need to be filtered out of the measurements. Since the effects are not very large and sudden, they can easily be seen in the videos. To make sure that these disturbances do not interfere with the measurements, the videos should be checked for these sudden disturbances before using them to extract data.

Secondly, the fluid is evaporating due to the heat of the lamp. As a droplet evaporates, particles in the fluid will be pulled to the edge. Here they will create a ring-shaped pattern. This process is known as the coffee-ring effect [27] and will cause a fluid flow in the droplet. Fluid will evaporate at the edge of a droplet and will be replaced by liquid from the interior. At the beginning of the coffee-stain process, the fluid flow will be quite slow, but as the droplet loses height due to evaporation, the process will accelerate and the fluid flow will increase.

Furthermore, it is expected that there are some big bundles of IRONSperm. These will also be sensitive to the magnetic field and therefore rotate or oscillate as well. During their motion, they will induce a fluid flow. This effect will likely be more prominent at higher frequencies and field strengths.

Finally, there is also an effect due to Brownian motion. Brownian motion is the random motion of particles suspended in a medium. It is the result of molecules bumping into visible particles. These collisions lead to

random motion.
Due to the random nature of the motion, the effect of Brownian motion is described by statistical equations. In two dimensions Brownian motion can be described by the following equation:

$$< r^2 >= 4Dt \tag{30}$$

Here, <r> is the average travelled distance, t is the time between the measurements, and D is the diffusion coefficient. The diffusion coefficient is dependent on the temperature and drag coefficient and can be defined as follows:

$$D = \frac{kT}{f} \tag{31}$$

Here, k is the Boltzmann constant, T is the temperature and f is the drag force. Assuming that the particles are spherical, the drag can be determined by the following formula.

$$f = 6\pi\eta a \tag{32}$$

Here a is the radius of the sphere and η is the viscosity of the fluid.

Initially, the idea was to even out the fluid motion by taking a reference point in each measurement and comparing the displacement of the reference with the displacement of the sperm cell. Subtracting the displacement of the reference particle from the displacement of the IRONSperm would then result in a compensated speed.
It is expected that there are a lot of particles of for instance dust that can be used as a reference. To find a suitable particle, there are some requirements that should be fulfilled;

- The reference particle should be visible in both the first and last frame of the measurement.
- The reference particle should not experience a magnetic torque.
- The reference particle should be far enough from the flagellum that its motion is not due to the flow generated by flagellar motion.
- The reference particle should be able to move, therefore it should not be stuck to the glass container or a result from dirt on the lens or camera.

However, this method can only work if the Brownian motion is negligible. If the particles are moving due to Brownian motion, reference particles can not be used to compensate for the moving fluid. In that case, the movement of the reference particles will not only be due to fluid motion but also a random motion due to the collisions with the water molecules. Subtracting the movement of the reference particles will then not result in accurate results.

To prove if Brownian motion is large enough to have a relevant effect on the reference particles, the motion of the reference particles will be analyzed. Due to the random nature of Brownian motion, particles subjected to it will move randomly and therefore not all in the same direction. If it can be observed that 2 reference particles take a very different path during one measurement, that is an indication that Brownian motion is occurring.
If the background fluid is moving due to a different reason, such as for instance evaporation, the entire droplet will experience this effect and therefore all particles will move in the same direction.

It will likely also be possible to see Brownian motion happening in the videos. If Brownian motion is significant, observing the movement of a reference particle will show a random motion. The particle will move in all directions, and its movement will not be explainable by simple fluid flow. If this observation can be made, it also shows that Brownian motion is significant.

If the results show that Brownian motion is significant, the above described method of compensation with reference particles will only introduce more uncertainty in the results. In that case; reference particles will not be used to compensate for fluid flow.

5.7 Measurement protocol

To gather data, two different experiments have been executed on responsive IRONSperm, the first is to determine the speed of the samples at different field properties and the second is to determine the step-out frequency of the sample.
Initially, the idea was to find a suitable swimmer and make this swim upwards to get away from non-responsive cells and prevent it from getting stuck at the bottom. However, this has been found to be very difficult. Due to the low swimming speed of the IRONSperm samples, gravity pulled them downwards quicker than they could swim upwards. Therefore, this approach has not been used. Instead, samples that were found to be responsive to the magnetic field were actuated in plane and steered away from the other cells.

In all experiments, once a swimmer had been found. Video recordings were made, so that the data could be extracted later. The videos were shot at 45 frames per second.

5.8 Analysis of the swimming speed

To measure the swimming speed of the IRONSperm, the videos are divided into frames. For a certain measurement period, the field strength, frequency and direction of magnetic field stay the same. Before each measurement period, the magnetic field is aligned, so that the best field is rotating in the plane perpendicular to the swimming direction of the IRONSperm. Furthermore, the sample is positioned so that the swimmer is in

the center of the image. During the measurement, the focusing depth is changed because the swimmer is sinking.

In the first and last frame of the measurement period, the tip of the head of IRONSperm are selected using the MatLab function ginput. The distance between the tip of the head of the spermcell in both frames is then calculated. This is done using Pythagoras' theorem, The travelled distance is thus defined as:

$$\text{distance} = \sqrt{(x_2 - x_1)^2 + (y_2 - y_1)^2} \tag{33}$$

In this equation, x_2 and x_1 are respectively the final and initial horizontal positions. y_2 and y_1 are respectively the final and initial vertical positions. The calculated distance will be compensated for fluid motion with reference particles if the effect of Brownian motion is not significant, else this distance will be directly used to calculate the speed.

To determine if there is a relation between the magnetic field strength and the swimming speed, the speed of a swimming sample will be measured in the case where the frequency is constant and the magnetic field strength is variable. The value for the frequency is chosen to be constant at 0.2 Hz. This value is chosen because it is very low and will therefore likely below the step-out frequency. Therefore, the sample will be able to complete full rotations at all values of the field strength. The difference in speeds will then not be caused by the step-out frequency.

The swimming speed is determined for multiple frequencies. For this, the magnetic field strength stays constant for each measurement. The value of the magnetic field is chosen to be 7mT. This is the highest value that can be used without risk of overheating the coils of the Helmholtz. A high field strength is beneficial because it is expected that the step-out frequency is higher for stronger field strengths. Measuring at a higher field strength will therefore allow for a larger range of frequencies and therefore more data points before the step-out frequency.

5.8.1 Error estimate

Although the data will be analyzed as accurately as possible, an error in the analysis will undoubtedly appear. This error is due to inaccuracies in selecting the tip of the head.
To estimate this error, the distance between the tip of the head and the furthest pixel that could be misinterpreted as the tip of the head has been measured. This distance has been found to be 10 px. Therefore the largest possible error in the travelled distance of the IRONSperm is 20 pixels. This is assuming that in the first frame, a pixel that was 10 pixels in front of the tip was selected, and in the last frame a pixel was selected 10 pixels behind the head was selected.

This error is multiplied with the conversion factor from pixels to μm, and then divided by the time. The time intervals varied for each measurement, this results in a varying error estimate as well. Measurements that have been taken over a longer period of time have a smaller error.

5.9 Step-out frequency

The frequency response is characterized by closely looking at the swimming pattern of the sperm cell. To obtain the step-out frequency at different field strengths, first a swimming sample had to be found. This sample would then be actuated at a low field strength and frequency. The frequency would then be increased with steps of 0.1 Hz to above the frequency where the step-out frequency seems to occur. At the step-out frequency the external magnetic field rotates too fast for the IRONSperm to keep up. The IRONSperm will then not be able to complete the full rotation simultaneously with the magnetic field. This will be visible in the videos because the movement of the IRONSperm will no longer be continuous. The sample will move for a part of the rotation and then stop for a short period until the magnetic field is again close enough to exert enough torque to promote rotation.

The frequency is increased to a value that lays above the frequency which is thought to be the step-out frequency during the experiment. The experiments are recorded and the datapoints are extracted from the videos. This is done because it allows for re-watching, pausing and playing the video at lower speeds, which makes the determination of the step-out frequency more accurate. If it becomes evident from the video analysis that the step-out frequency occurs at higher frequencies than was thought during the experiments, it is necessary to have videos of a higher frequency as well.

The frequency can only be increased with steps of 0.1 Hz. Therefore, there is a quite large error in the measurements of the step-out frequency. There are no data points between the steps, so the real step-out frequency could be lower than the data point. The step-out frequency in the results is defined as the first point where the IRONSperm does not continuously rotate with the magnetic field anymore.

6 Results

6.1 Observation method

An overview of the advantages and disadvantages of both the hanging droplet and the container has been summarized in table 1. As can be seen from the table, the hanging droplet had more disadvantages and the container shows to be more advantageous. Therefore all measurements have been taken using the container.

However, the disadvantage of IRONSperm sticking to the bottom remains. This is an important experimental limitation because it limits the amount of swimming IRONSperm. The hanging droplet however showed a new disadvantage which had the same consequence. In the hanging droplet, the cells did not stick to the glass plate, but instead they are accumulated in the bottom of the droplet as can be seen in figure 5a. Here, the IRONSperm clusters and the flagella become intertwined. This results in the same issue as with the container, after some time the samples have sunken due and become useless.

The hanging droplet also had some other disadvantages compared to the container. It was more sensitive to disturbances from sources outside the setup. Events like a closing door resulted in a visible disturbances in both cases, but the effects were visible for longer in the hanging droplet. The same was true for measuring at high frequencies. High frequencies resulted in an oscillating image in both setups due to oscillating bundles, but the effects were more prominent in the hanging droplet.

Finally, the hanging droplet was just generally more difficult to work with. It was more difficult to prepare the droplet. Also, focusing the microscope on the hanging droplet was more difficult as the droplet made it impossible to get samples at the edge in focus and resulted in images as shown in figure 5b. That is why for all measurements, the container was used.

To overcome the problem of cells sticking to the bottom, only the IRONSperm that were not stuck were used. There were enough that could be used to obtain results.

6.2 Fabrication method

As described in section 2.1, multiple approaches to making IRONSperm were used. All three fabrication methods have been experimentally observed.

The method which has been used to promote bundling by selecting the spermcells with the largest swim-up times, before adding the iron-oxide particles worked, but was not useful in the research to multi-flagellar IRONSperm. Indeed, there were a lot of bundles, but instead of bundles at the head which would result in multi-flagellar IRONSperm, the bundles consisted of many IRONSperm clustered together. An image of one of these bundles can be found in figure 6. These bundles consisted of IRONSperm connected on multiple locations. Some of the IRONSperm in the cluster would react to the applied magnetic field, but they were stuck in the cluster so they could not freely swim. This fabrication method did not yield any multi-flagellar IRONSperm. Therefore, it was not useful to use samples fabricated this way, because they were unable to create multi-flagellar IRONSperm.

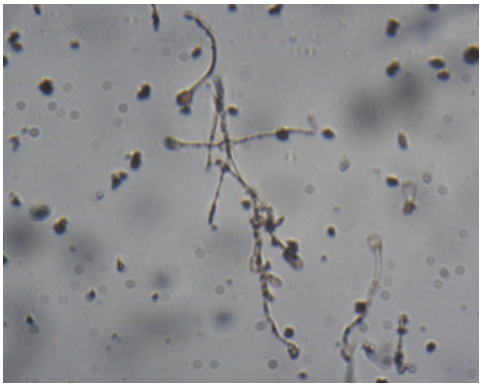

Figure 6: IRONSperm that has been fabricated by selecting the sperm-cells with the largest swim-up time form bundles by connecting at random locations. These bundles consist of both actuatable and non-responsive IRONSperm. This image has been taken in the container with the 20x lens.

Table 1: Overview of the advantages and disadvantages of the hanging droplet and the container method

	Advantages	Disadvantages
Container	• Easy to use • Less sensitive to disturbances • Easier to focus microscope	• IRONSperm sticks to the bottom
Hanging droplet	• Cells can not stick to the glass	• Cells clutter at the bottom of the droplet

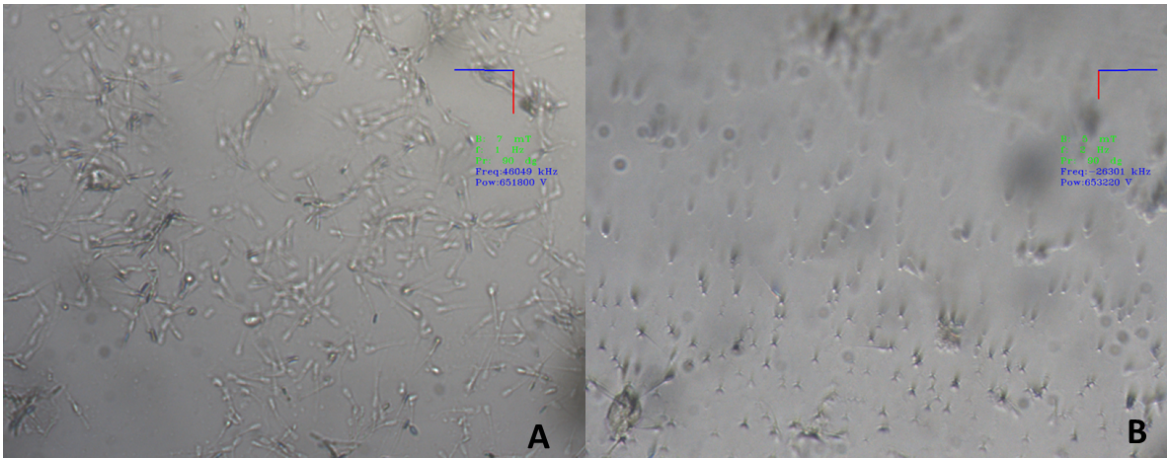

Figure 5: A) shows the bottom of the hanging droplet. As can be seen, IRONSperm cells have sunk to the bottom where they collided with other IRONSperm. Due to this collision, clusters of IRONSperm have been formed and it is no longer possible to analyze a single IRONSperm. B)Cells at the edge of the hanging droplet could not be brought into focus. This resulted in images that appeared to have stretched cells. This effect occurred in both the hanging droplet and the container but the effect in the hanging droplet was worse. Both images have been taken in the hanging droplet with the 10x lens.

The second method that was used in attempt to fabricate multi-flagellar IRONSperm was the method of using Spinell particles. This fabrication method also did not prove to be useful in creating multiflagellar IRONSperm. Although there were some bundles, most IRONSperm was singular and did not bundle. In the entire sample, no example of multiflagellar IRONSperm was found. In addition to that, IRONSperm that had been coated with spinell particles showed a less strong magnetic response. Although there were some examples of single-flagellar IRONSperm in the sample, their response to the magnetic field was worse than for the samples produced with rice-grain maghemite. Therefore, these samples were not used for further analysis.

Because no multi-flagellar IRONSperm were found, it was not possible to compare the swimming mechanisms of single-flagellar IRONSperm to multi-flagellar IRONSperm. To research the effects of the magnetic field parameters, IRONSperm that has been coated with iron-oxide rice particles has been used.

6.3 Prove rotation

To correctly interpret the data, it is important the the way of movement is interpreted correctly. Figure 7 shows one full beat cycle of an IRONSperm sample. This sample had a hook at the end of the flagellum. By studying the motion of this distal end, it can be seen that the sample performs a three-dimensional rotation.
Secondly, the head also shows rotational movement. If the IRONSperm would be moving with an oscillatory 2D movement instead of a rotational 3D movement, the shape of the head would stay the same in all frames. In that case, the angle that the head makes would alter, but the orientation of the head with respect to the camera would stay the same. As can be seen in figure 7 and 16, the shape of the head changes as the field rotates. This is an indication that the head is rotating because the dimensions of the head are not the same from every angle.

Finally it can also be seen that the colour of the flagellum changes while it is being actuated. One example of this can be seen in figure 16. In the 3rd frame the amplitude is pointing towards the observer. In the 6th frame, the amplitude is pointing away from the observer.

Figure 7: This set of images shows an IRONSperm sample with a distinct hook-structure at the distal end of the flagellum. The images show the IRONSperm for one full rotation. The images are taken with a magnification of 880 times. There is 0.4 seconds between each consequitive frame.

It can be seen that the flagellum is darker in colour in the 3rd frame than in the 6th frame. This is an indication that the flagellum is moving out of focus of the microscope and therefore executing a three dimensional movement.

6.4 Prove flexibility

The flexibility can be quantified by the effect of the actuation frequency on the envelope of motion. The wave amplitude of a flexible filament decreases with an increase in actuation frequency, while a rigid flagellum does not show a change in wave form.

The flagellar amplitudes are measured when the largest deformation is pointed towards the right as in figure 8. They have been measured at 4 different frequencies; 0.5 Hz, 1 Hz, 1.5 Hz and 2 Hz. Closely looking at this figure shows that the flagellum has the same shape in all pictures. The wave of the amplitude has been measured in 3 different frames for 4 frequencies (0.5 Hz, 1 Hz, 1,5 Hz, and 2 Hz), figure 8 shows 1 of these frames for each frequency. It has been found that the height of this amplitude is 5,7 $\pm$ 0.2μm in all cases. Therefore, the flagellar amplitude of the IRONSperm does not change which is an indication of a rigid flagellum.

To further support this finding more evidence is needed as the measurement of the flagellar amplitude contains a considerable error. Another piece of evidence that arguments for a rigid flagellum can be found in figure 7. In this IRONSperm the distal end of the flagellum was hook shaped. Frames of a video where this sample performed a full rotation, show that this hook shape stays for the entire rotation. This hook-shape is a shape that is unlikely to form in a flexible flagellum due to viscous forces acting on the shape, which will push it to bend straight. Also, this shape stayed the same for all frequencies and field strengths.
Finally, the IRONSperm also shows rigid behaviour when rotated in plane. By applying a gradient field instead of a rotating field, the IRONSperm could be rotated in plane. The result of this experiment can be found in figure 9.

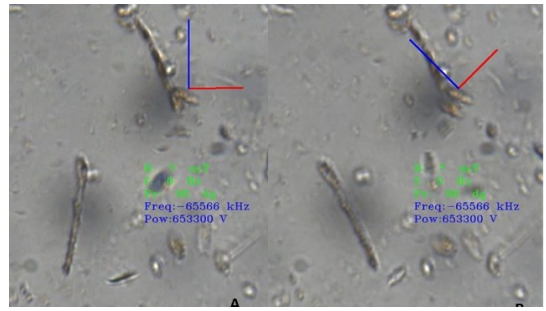

Figure 9: A responsive IRONSperm is exposed to a gradient field that is in plane with the image. The field is rotated with 45 degrees and the IRONSperm rigidly rotates to its favoured position again. The time between the frames is 16 seconds.

For a flexible flagellum, it would be expected that rotating the IRONSperm in plane would result in the flagellum curling around the sperm-head. It can be seen in figure 9 that the IRONSperm rotates as a straight object and does not deform during rotation. This is also indicative of a rigid flagellum.

6.5 Orientation with respect to the magnetic field

The experiments show that IRONSperm swims perpendicular to the rotating magnetic field. In the images, the axis which is perpendicular to the rotation and thus the swimming direction is the blue line.
At relatively high frequencies, the IRONSperm misalligns with respect to the magnetic field. The IRONSperm deviates from the blue line and starts moving in a different direction. This happens without changes in the conditions, the field strength, direction and frequency of the magnetic field are not changed but the swimming direction of IRONSperm does change. Screenshots of a measurement in which this occurred can be seen in figure 10.

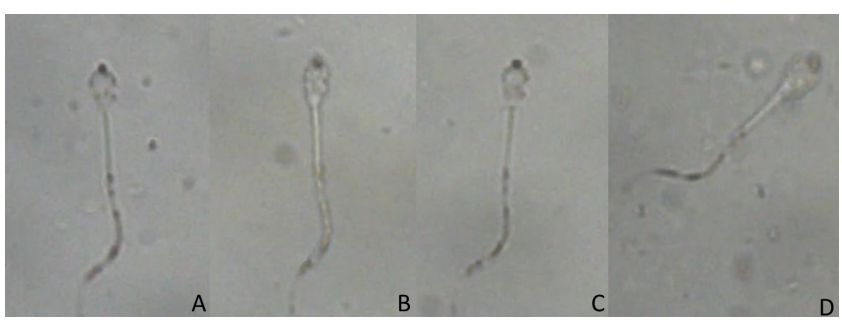

Figure 8: Screenshots from which the flagellar amplitudes are determined, every measurement was done at 7mT. The frequency was variable, A) 0.5 Hz B) 1Hz C) 1.5 Hz and D) 2 Hz. Although the IRONSperm has been rotated at 2Hz, the flagellar wave shape is the same for all frequencies.

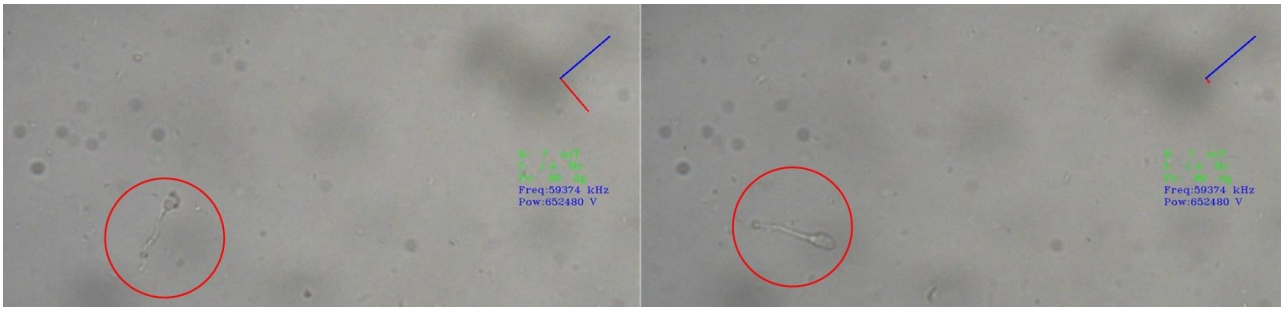

Figure 10: Two images of an IRONSperm that are taken 7 seconds apart. The external magnetic field had a field strength of 7mT and a frequency of 1.3 Hz for the entire measurement. The sample clearly deviates from its swimming line. In the time between these two frames, no changes were made to the parameters of the magnetic field.

Secondly, an experiment with a gradient field was executed. In this experiment, the field was not rotating so there was only a gradient. Rotating the direction of this gradient with 45 degrees in plane resulted in the rotation of the sample. This experiment can be found in 9. Changing the angle of the magnetic field, resulted in an in-plane rotation of the sample.

From this experiment the in-plane rotational speed can be determined. The time between the frames is 16 $\pm$ 1 seconds. In this time, the sample has turned with 45 degrees. Therefore the rotational speed is 2.8 $\pm$ 0.2 degrees/second.

It was expected that the IRONSperm would align itself with the red line which depicts the direction of the magnetic field. This was expected because in that case, the magnetic torque would be minimized according to equation 19. However, it can be seen that the sample does not align with the red line.

There are multiple possible explanations why this could be happening. Firstly, the IRONSperm could be influenced by the earth magnetic field. If that is the case, the sample would experience an additional magnetic torque and therefore have a different position where the net torque is 0. However, if the earth magnetic field would have a considerable effect on the samples, this would be visible when turning off the Helmholtz coils. Then, the total magnetic torque would change and the samples would rotate to align with the earth's magnetic field. Furthermore, it would then be expected that all samples with a high enough magnetic moment would position themselves in the same way. Both of these effects have not been observed and therefore it is unlikely that the earth magnetic field is the explanation for this type of alignment.
Another explanation lies with the direction of the magnetic moment vector. It has been assumed that the magnetic moment lays along the long axis of the IRONSperm. However, it could be possible that the magnetic moment is in reality pointed in a different direction.
The magnetic moment results from the rice-grain shaped particles. These particles are ellipsoidal shaped. The long axis of an ellipsoid is the easiest axis to magnetize [28]. Therefore, it will be most likely that the angle between the magnetic moment of the nanoparticles and their long axis is small.
The nanoparticles attach to the IRONSperm mainly with their long axis along the long axis of the sperm. Although the magnetic moment vector will not lay exactly along the length of the IRONSperm due to agglomerates of nanoparticles, the angle between the magnetic vector and the long axis will be relatively small. Therefore, this can not be the only reason for the way of alignment of IRONSperm to the external magnetic field.

The most likely explanation is that the alignment of this IRONSperm is due to a large drag torque. Rotation occurs if there is no balance in the torques. On this IRONSperm, 2 torques are applied. The magnetic torque as is described in equation 19 and a drag torque that is dependent on the geometrical parameters, viscosity and speed. When these two torques are in equilibrium, the IRONSperm stops rotating.

The IRONSperm is in this case stationary at a angle of almost 90 degrees between the long axis and the direction of the gradient field. This angle causes an almost maximal magnetic torque, which is why the drag torque must also be very high. This high drag can follow from the shape of the IRONSperm. Due to the shape of an IRONSperm, the drag torque when rotating the IRONSperm along its long axis is much smaller than the drag torque to rotate the IRONSperm in plane.

6.6 Fluid motion

As described in section 5.6, there will likely be fluid flow in the droplet. To check if Brownian motion occurred, the movement of 2 reference particles were compared to each other. The screenshots that were used for this can be found in figure 11. The time between the two images

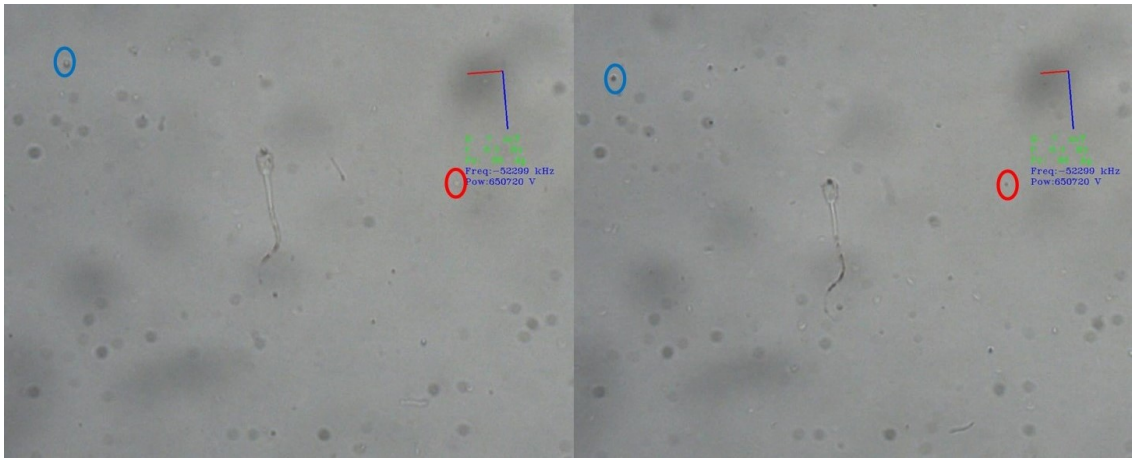

Figure 11: Two particles are analyzed to find if Brownian motion is significant. The travelled distance is measured for both particles. In case of Brownian motion these direction of movement would not be the same as the particles moved in a random pattern. The time between the two frames is 14.2 seconds.

Table 2: Overview of distance of the two reference particles that are shown in figure 11.

	Motion vector (μm)	r^2
Circled in Blue	$\begin{bmatrix} 9.3 \pm 2 \\ 0.1 \pm 2 \end{bmatrix}$	9.3 ± 2.8
Circled in red	$\begin{bmatrix} 7.2 \pm 2 \\ 1.2 \pm 2 \end{bmatrix}$	7.3 ± 2.8

was 14.2 seconds. The measured distances of the particles can be found in table 2.
The errors in the values are very large compared to the distances. This is because the used method was not very precize and the particles did not travel far. The value of r, which is the total travelled distance is different for both samples. Equation 30 shows that the travelled distance is linearly dependent on D. Because all other conditions were the same for both particles, r should be linearly related to $\sqrt{a}$. In that case, the found values show that the blue particle is larger than the red particle. However, again the uncertainty in the data is too large for the data to be considered trustworthy.

However, Brownian motion can still be seen in the videos. When following a particle in the background it is clear that the particle moves randomly. It moves in all directions and there is no clear pattern or fluid flow that can prove this. Therefore, Brownian motion will influence the measurements. The measurements on swimming speed will thus not be compensated using reference particles.

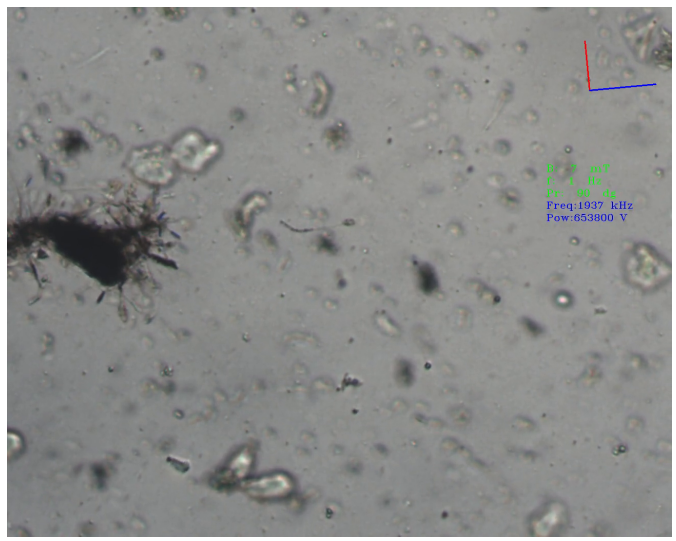

Figure 12: A swimming IRONSperm and a bundle of IRONSperm are captured in the same image. Both the bundle and the IRONSperm swimmer are responsive to the magnetic field. The bundle oscillates with the magnetic field and generates a fluid flow that will influence the swimming speed of the IRONSperm and adds an error to the measurements.

6.6.1 Bundles

As was expected, there were a lot of large bundles of IRONSperm present in the sample. One example of a bundle can be found in figure 12.
Most of these bundles were responsive to the magnetic field. Therefore they also moved when the magnetic field was applied which created fluid flow. These effects were worse at high frequencies and field strength, and result in very shaky videos. Furthermore, these fluid flows will also interfere with the measured swimming speed of the IRONSperm.

6.7 Field strength

As described in section5, the recorded videos were divided into frames, from which the swimming speed was extracted. The swimming speed at different field strengths, can be found in figure 13.
To fit a line through the data points, a line of the zeroth order has the least error. The best fit through the data points is shown in figure 13 including its root mean square error. The point through (0,0) has not been taken into account when making the linear fit line. This is done because the actuation is a step response. Therefore, although the speed is 0 at 0 mT, it has not been included in the linear fit.

From the results, it becomes evident that there is no clear increase or decrease in swimming speed of IRONSperm. Although there is variation between the swimming speeds at different field strength, there is no increasing or decreasing trend visible in the swimming speed. The trendline shows that there is great variation in the data. Even when taking the error margins into account, not all data fits on the horizontal line line. It is most likely that this is a direct result from inaccuracies in the measurement method. For instance, the way that the distance is measured or that there is no compensation for fluid flow.

6.8 Frequency response

The effect of the external frequency has been researched in a similar fashion to that of the field strength.
Figure 14 shows the velocity of a different swimming samples at a range of frequencies. It was expected that the speed would increase with an increase in frequency, up to the step-out frequency, after which the speed would drop.

The sample from which the frequency response has been measured plotted on the left of 14 had a step-out frequency of 1.3 Hz. As can be seen in the figure, the speed is indeed a lot smaller after this frequency.
To find the trend in the data, MatLab function polyfitZero of the first order was used on the data points before the step-out frequency of 0. This function finds the best fitting line through the data points that goes through zero. As can be seen in figure 14 there is an increasing trend for the points before the step out frequency.

For the datapoints after the step-out frequency, a first order linear fit was also made. This linear fit showed a linear decrease in speed, although this effect is relatively small especially compared with the velocities before the step-out frequency.
The errorbars in the frequency response are quite large. As explained in section 5.8.1 this is due to errors in selecting the right pixel. Since the duration of the measurement varied per frequency, the error bars are of varying size. Compared to the difference in speed from increasing the frequency, the error is very large. Therefore, it is more difficult to draw conclusions from this research.

The same analysis has also been carried out on another sample. That frequency response is shown in figure 14 on the right.

It immediately becomes evident that these results are very different from the first frequency response, this is unexpected because the step-out frequency was the

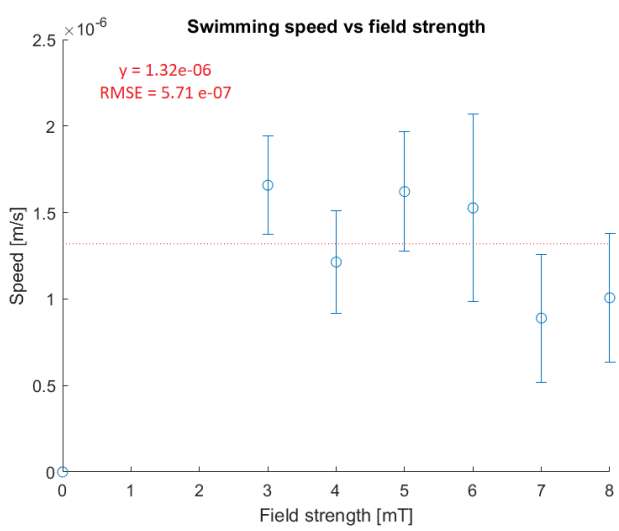

Figure 13: The swimming speed of a sample at different field strengths. The magnetic field had a frequency of 0.2 Hz and a field strength in the range of 0 to 9 mT. MatLab function polyfit has been used to find a fit of the zeroth order for the datapoints. The best fitting line was the horizontal line at 1.32 μm/s. The root mean square error (RMSE) of the fit was 5.71

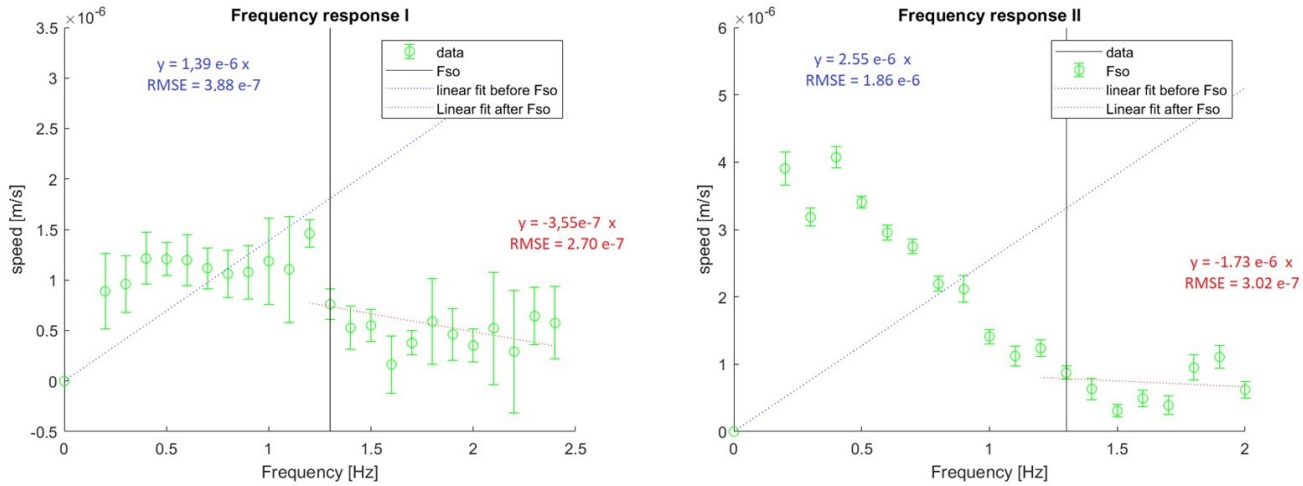

Figure 14: The frequency responses have been obtained for two IRONSperm. Both IRONSperm had a step-out frequency of 1.3 Hz. For both graphs, 2 linear trendlines have been fitted, one before and one after the step-out frequency using MatLab polyfit.

same for both samples, and therefore their magnetic moments are likely similar as well. The speeds in the beginning of frequency response II are very high and decrease before the step-out frequency. There is also a less significant drop in speed after the step-out frequency, when compared to the other sample. Finally, the speeds vary a lot both before and after the step-out frequency.
The most likely explanation for the unexpected response to increasing the frequency can be found by analyzing the fluid flow. Figure 15 shows the overlay of two different measurements of the experiments. Both are of frequencies below the step-out frequency. It is very clear to see that at 0.2 Hz, the IRONSperm has also travelled a large distance . It is unlikely that this movement is result of flagellar thrust. Flow of the fluid is a likely explanation for this phenomenon.

As a result of the used method for determining the distance of the IRONSperm, the movement that is not in the swimming direction is also incorporated in the distance and therefore the speed. This would likely explain the remarkably high speeds at low frequencies. As can be seen in figure 15. There is no compensation for moving fluid, and therefore the measured speed in the frequency response is very unreliable.

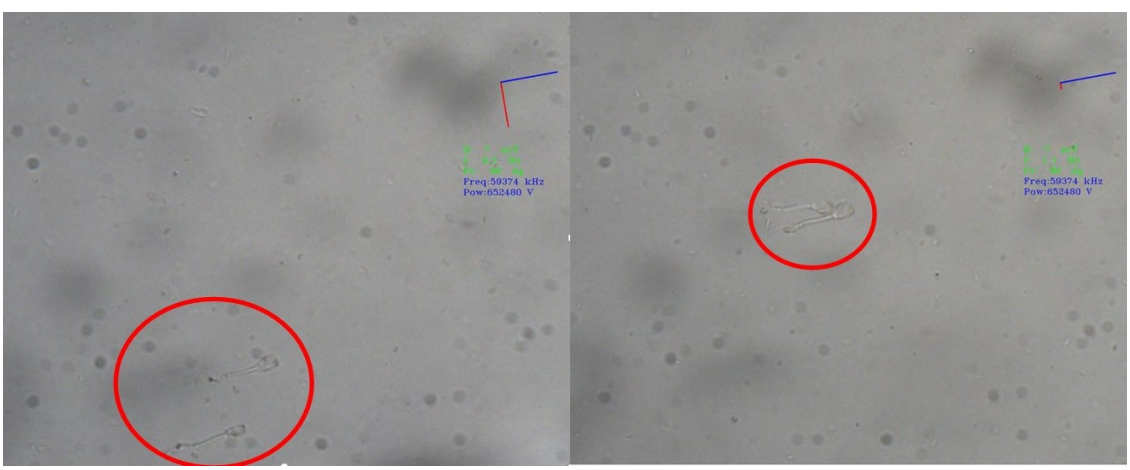

Figure 15: This figure shows the overlay image of the IRONSperm from which the frequency response is obtained. The IRONSperm is actuated with a field strength of 7mT and a frequency of 0.2 Hz (figure A), or a frequency of 1.1 Hz (figure B). At 0.2 Hz there is a lot of movement in the y-direction which is not the direction of the flagellar propulsion. This movement is likely a result of fluid flow and is a lot less prominent at 1.1 Hz.

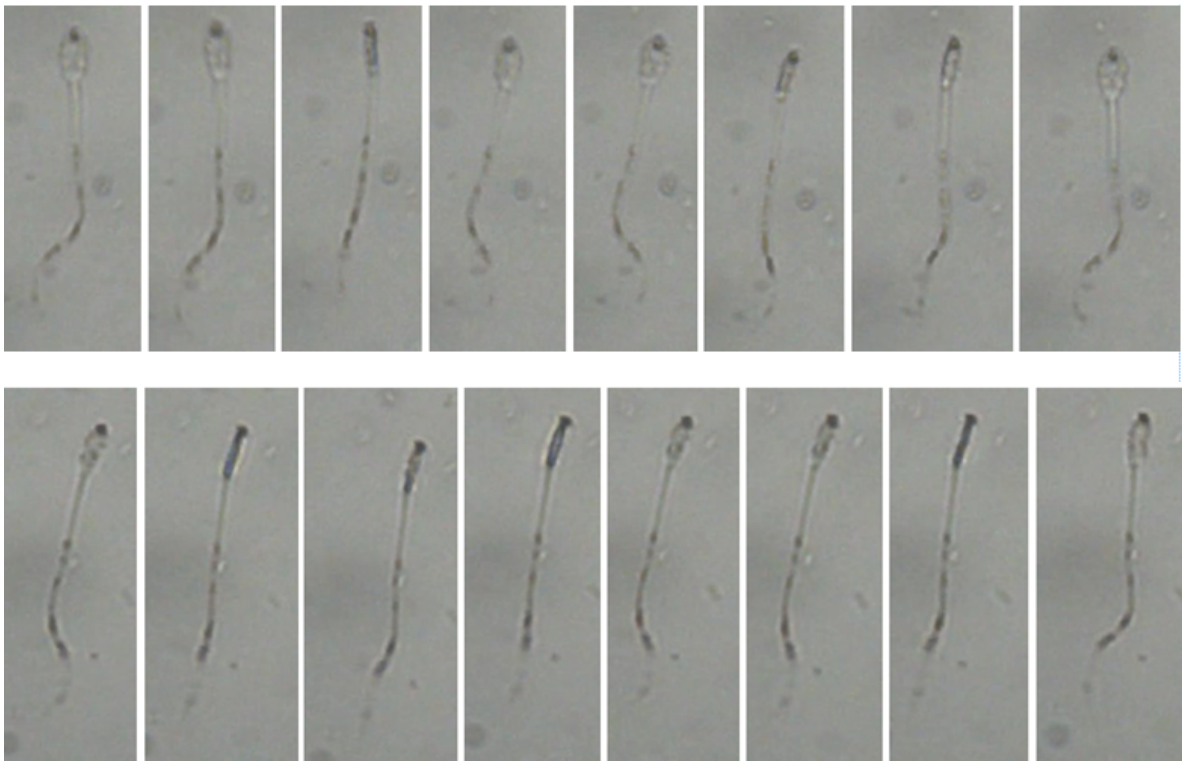

Figure 16: This figure shows the swimming pattern of the IRONSperm from which the speeds in figure 14 was created. The IRONSperm was actuated with a field strength of 7mT. For the top row, the frequency of the external magnetic field was 1.2 Hz. This frequency was below the step-out frequency. It can be seen that the IRONSperm continuously rotates with the field. The bottom row consists of frames of the same IRONSperm actuated at a frequency of 1.3 Hz. This frequency is above the step-out frequency. Here, it can be seen that the IRONSperm is no longer continuously moving but instead swims with a more jerky movement. All images are taken with the 20x lens. The time between two consecutive frames is 0.06 seconds.

6.9 Step-out frequency

The swimming pattern of IRONSperm has been studied to find at which frequency, they can no longer follow the magnetic field. At this frequency, the swimming pattern becomes very different. The differences in swimming pattern are shown in figure 16. As was expected there is a clear distinction in pattern for actuation frequencies above and below the step-out frequency. Below the step-out frequency, which for this IRONSperm is 1.3 Hz, the IRONSperm showed a continuous rotation.

Above the step-out frequency the IRONSperm no longer continuously rotates. Instead the IRONSperm shows a jerky motion, where it rotates a bit, stops moving for a while and then rotates a bit further. The lower row of figure 16 illustrates this movement. As can be seen, the IRONSperm rotates very little between frame 2,3, and 4 of the bottom row. Especially when it is compared to the rotation at 1.2 Hz, the rotation is clearly not continuous.

The step-out frequency has been determined at different strengths of the external magnetic field for 4 samples. As a linear fit was expected, the MatLab function polyfitZero of the first order has been used to find a linear relationship between the data. This function finds a trendline that minimizes the root mean square error and goes through zero. The line has been forced through (0,0) because it is known that the step-out frequency must be 0 at 0 mT.

The characterized step-out frequencies are shown in figure 17. As discussed before, the errors are quite large. It can be seen that there is large variability in step-out frequency for different samples. IRONSperm B for instance shows very low step-out frequencies in comparison to the other IRONSperm. At 5 mT IRONSperm B had a step-out frequency of 0.2 Hz while all other IRONSperm had a step-out frequency of 0.8 Hz at 5mT. It was expected to see large variability in the step-out frequencies of IRONSperm with the expectation that there is variability in the magnetic moment of different IRONSperm.

The results show that there is indeed a increase in the step-out frequencies at higher field strengths. The gradients of the linear fits are different for all IRONSperm, but as can be seen in 17 they are all positive which indicates an increase in step-out frequency with an increasing field strength.

The quality of the fitted line is expressed in the values of the root mean squared error (RMSE) which can be found in figure 17 For IRONSperm B, the RMSE is the smallest, this also corresponds with the visually best fitting line. Almost all datapoints of IRONSperm B fit on the line, eventhough the step-out frequencies of IRONSperm B stand out most from the rest and are very low. If the error bars are considered, all data of IRONSperm B fits on the line. The line of IRONSperm D is also a good fit. If the error bars are taken into account almost all datapoints fit on the line. However, the points at 4 and 9 mT do not fit on the line even with their error. IRONSperm A also shows a relatively good correspondence with the linear trend. Here only the datapoint at 6mT does not fit on the line if the error bars are considered.
The data of IRONSperm C does vary a lot from the linear fit. As explained this could be due to the large error in the data, but even if the large error bars are taken into consideration, there is still no possibility of a line that goes through all the points. This is mainly due to the fact that there the data point at 6mT and at 9 mT are not in line with the other points. The most likely explanation for these variation either lies with observational errors. It could also be that the IRONSperm got stuck during the measurement, which would also result in a jerky motion that could be misinterpreted as the step-out frequency.

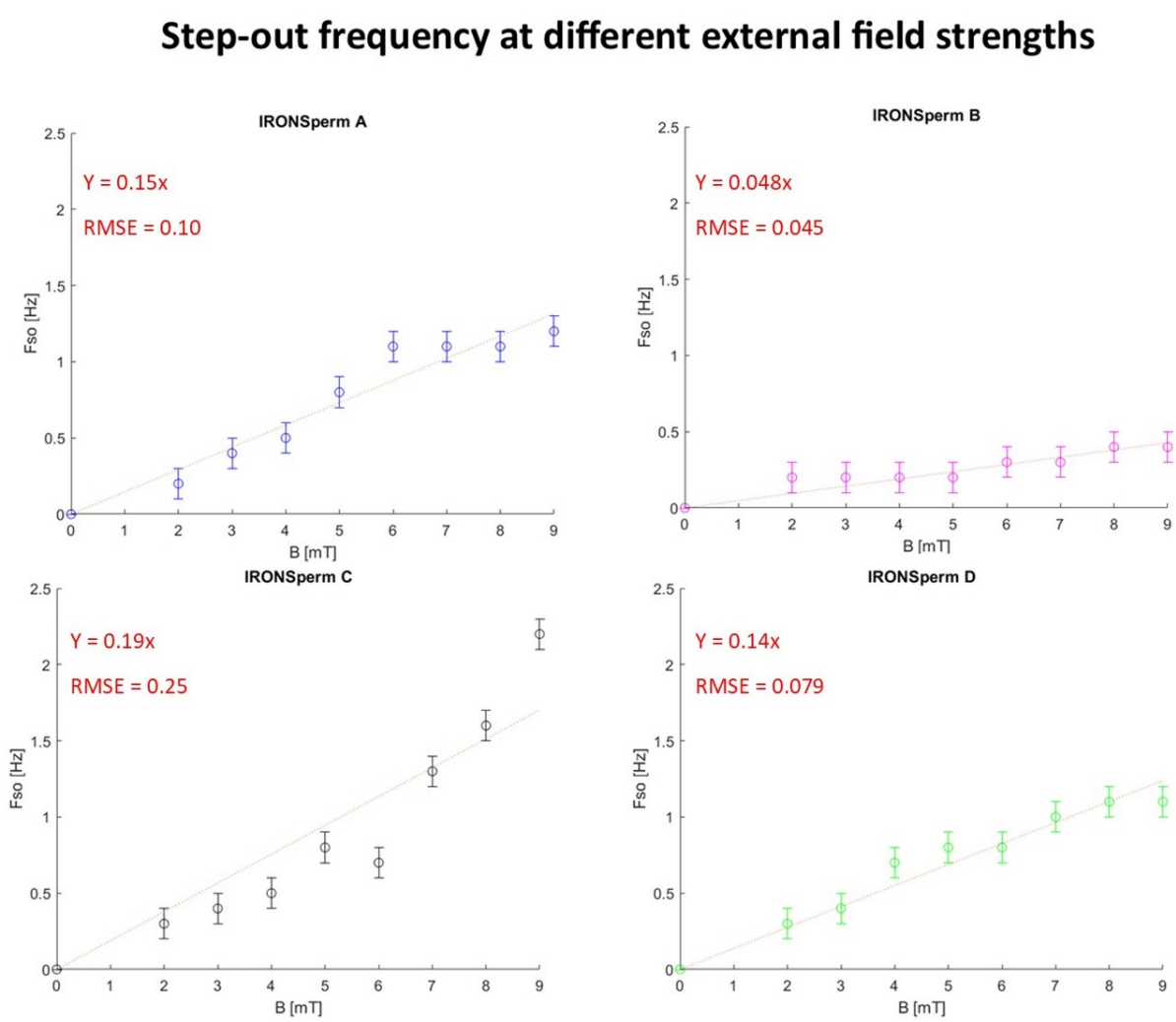

Figure 17: The step-out frequencies are obtained from 4 different swimming samples at different field strengths of the external magnetic field. The step-out frequencies are plotted and evaluated with a linear fit that is created using MatLab polyfitZero.

7 Discussion

7.1 Cell to cell variability

As expected, a large cell to cell variability was observed. The majority of the IRONSperm were not actuatable with a magnetic field. A large sample variability is a logical consequence of the fabrication method. The method of electrostatic self assembly, is based on the charge of the sperm cell which varies with the developmental stage and will therefore be different for different samples. Due to this fabrication method, not all samples receive the same amount of nanoparticles and therefore not the same magnetic moment. The sample variability also becomes evident from the differences in step-out frequency. Especially comparing step-out frequency B to step-out frequency D, shows a large difference which is likely due to a difference in magnetic moment.

There were a lot of samples that were not responsive to the magnetic field at all. This caused trouble in the experiments, because these sperm cells still added clutter in which swimming IRONSperm could get stuck. This is also something that happened while conducting measurements, which made it difficult to obtain complete frequency responses.

7.2 Magnetic segmentation

In this research the effect of the place of the magnetic particles has not been studied. As explained in section 2.2.2 the position at which the nanoparticles adhere to the spermcell have an effect on the flagellar wave. However, since the studied samples are rigid, the waveform can not change. Therefore, the locations of particles does not have such a strong effect during swimming.

The effect of magnetic segmentation on rigid swimmers is much lower as the waveform does not change. However, the distribution of particles might influence the shape in which the flagellum gets stuck. Therefore, it is of interest to research the distribution of nanoparticles along the IRONSperm because it might be a cause of high variability in swimming speeds.

7.3 Low swimming speeds

The samples from which the frequency response was obtained showed a swimming speed that is much lower than was expected. Earlier research on IRONSperm [5] has shown swimming speeds that exceed 6.8 μm per second, but the highest value that has been obtained in this research lays around 4 μm per second and that value is heavily influenced by fluid flow. The highest swimming speed that is likely not heavily influenced by fluid flow is approximately 1.5 μm.

It should be noted that the swimming speeds in earlier research on IRONSperm have been obtained with a cone angle, which is the angle that the magnetic field makes with the axis around which is rotating, between 45 and 60 degrees. In this research the cone angle was 90 degrees for each measurement. It has been shown that swimming speeds of magnetic microrobots are maximum when the cone angle is 90 degrees. Therefore it is unlikely that the cone angle is the reason for the low swimming speeds.

The most likely explanation for the low swimming speeds is that the magnetic moment is a lot lower in this samples. The values from earlier research in IRONSperm [5] were obtained at much higher frequencies. It is to be expected that these higher frequencies also resulted in higher swimming velocities. However, the IRONSperm in this research had a lower step-out frequency and therefore could not effectively swim at higher frequencies. This conclusion would also explain the relatively low step-out frequencies.

The low magnetic moment is a direct influence from the fabrication of the samples. The fabrication process is based on electrostatic-self assembly which is a process that is difficult to predict. The most likely explanation for the low magnetic moment is that the maghemite particles did not form as large agglomerates as in previous research. Therefore there are less large groups of nanoparticles attached to the sperm cell and the magnetic moment is lower.

Another possible explanation for the swimming speed, is that the swimming envelope of the samples is relatively small. The IRONSperm samples are rigid and therefore there will be no travelling wave in the flagella, as described in chapter 3. Instead, the shape of the flagellum is fixed. This fixed shape may more straight than it would have been if it were flexible. If that is the case, it becomes evident from equation 15 that the flagellum generates less thrust because $\frac{\partial y}{\partial x}$ is smaller.

7.4 Characterization of IRONSperm

To further explain the behaviour of IRONSperm, it would be very interesting to gather data of the samples. It would for instance be very interesting to have information on the magnetic moment of the sample so that the step-out frequency could theoretically be predicted. Then experimental data can be compared to experimental data. This also allows for testing if the low swimming speeds are indeed a result of a low magnetization.

7.5 Extraction of wave variables

This research can be expanded on by finding the theoretical velocities and thrusts with resistive force theory and comparing those to experimental observation. From experimental data, the wave variables of the flagellum can be obtained. These can then be used to find an expression for the tangent angle in the flagellum as explained in section 3.1. From here, the velocity and thrust force can be calculated.

This method is very time consuming as for every video frame, the flagellum will have to be traced to obtain the wave variables. However, it would be very interesting to compare experimental results with theoretical models, as this might lead to new insights in flagellar propulsion.

7.6 Experimental limitations

In this research, results have been obtained experimentally, which introduced some additional challenges.

7.6.1 Getting stuck

One of the major problems in the experiments, was that IRONSperm tends to get stuck to the bottom of the glass or in another bundle of IRONSperm. This made it very difficult to actuate an IRONSperm sample for a long period of time, because it would often get stuck to the glass, dust particles, or other IRONSperm during the measurement which resulted in incomplete measurements.

As described in the method section, the initial idea was to first move the samples away from the bottom of the container by steering the IRONSperm upwards. In the experiments this has been seen to be very difficult because the IRONSperm was swimming very slowly and therefore could not overcome gravity.
Also, bringing the IRONSperm upwards could also result in the cell getting stuck during the process. Due to the fact that it was quite rare to find a swimming sample it was decided to not take the risk to try to get the IRONSperm to swim upwards. The IRONSperm could very well be steered in plane, so it could be prevented from getting stuck. Still, it would be preferable to be able to bring the IRONSperm upwards because then it could swim more clearly and is also easier to see in images because there is less clutter.

There were also instances in which the IRONSperm stopped responding to the magnetic field for no clear reason. In those cases,it was not stuck to the bottom of the container or visibly swimming into something but it still stopped swimming at parameters of the magnetic field that had yielded actuation before. Probably the IRONSperm did get stuck to a particle that was simply not visible because it was out of focus. This occurred on multiple occasions and therefore made it difficult to gather full data-sets on frequency responses.

7.6.2 Small dataset

In an ideal situation, more data on the swimming speed of the samples would have been gathered. The current data set only contains one thrustworthy frequency response and therefore does not provide very strong evidence. It has been difficult to find IRONSperm from which the speeds could be extracted. Many IRONSperm samples were not be responsive to the magnetic field or were stuck. Also, sometimes the IRONSperm would stop moving after the first few measurements were done because it would run into another sample. This made it difficult to extract data from which a complete frequency response or graph of step-out frequencies could be made. To make the conclusions stronger, more data is needed to prove that IRONSperm indeed behaves as described in this research.

7.7 Inaccuracies in methods

Although it has been tried to obtain the results as precisely as possible, there are still inaccuracies in the results. In future research, the methods that have been described in this report can be improved on to obtain more exact results.

7.7.1 Flexibility

As described before, the samples have been found to be non-flexible. In this research, this has been done by measuring the amplitude of the wave at different frequencies. However, the accuracy of this method can be improved on. The measurements have been conducted by hand and therefore contain errors. Therefore, it could be possible that there is a small decrease in amplitude, which would be an indication of a flexible tail.

Due to the fact that the visual analysis also shows a rigid body, since the flagellum seems to show the exact same shape in every measurement, it can be concluded that the flagellum is rigid. However, to prove this even more, the flexibility can be determined more accurately by analysing the wave pattern. One way to do this, is by tracking the wave pattern in for instance MatLab. By tracing the flagellum the swimming envelope can be reconstructed. Doing this at different frequencies will result in being able to compare the swimming envelope, and therefore a more accurate way to see if the envelope decreases.
Furthermore the wave parameters can be extracted from a 2D projection of the flagellum. For a rigid body, the wave parameters would be the same in every situation. For flexible bodies, the wave parameters would change. If no significant change in wave variables occurs in the measurements, the observation of the rigid swimmer is strengthened even further.

7.7.2 Time of measurements

If the time between the measurements is increased, the error that is due to selecting the position of the tip of the head will decrease. Therefore, it is beneficial to have a long period for each measurement. However, as explained before IRONSperm has the tendency to get stuck or sink to the bottom of the container. Therefore, it is difficult to measure for very long.

To measure the swimming speeds over a longer period of time, the risk of the IRONSperm getting stuck should be minimized. This could be done by diluting the sample even more, so that there is more open space to swim. Furthermore, the IRONSperm could be actuated under a swimming angle, meaning that part of the propulsive force will counter the gravity. However, this method has the important disadvantage that the swimming speed in plane will decrease. The swimming speeds of IRONSperm are low and therefore decreasing the speed in plane is not desired. That is why for the conducted experiments, the field has been applied in a matter that will result in maximum propulsive thrust in plane.

7.7.3 Swimming speed

One of the most prominent approximations in analyzing the results was the way in which the speed was determined. As described in the method the speed has been determined for the case in which the IRONSperm would travel in a straight line. However, in reality the actual swimming speed would likely be higher because the IRONSperm would likely be moving in a curved path. It would be interesting to study different types of velocity to get a better understanding of the velocity and thus the propulsive thrust that is generated by IRONSperm. There are multiple ways that velocity can be determined. The first is the curvilinear velocity. This velocity describes the entire path that the IRONSperm takes. The second is the average path velocity which determines the average path. The final method is to determine the straight line velocity, which is based on the shortest distance between 2 points.

The curvilinear velocity and average path velocity both give more accurate results than the used straight line velocity. However, they also are much more time consuming to measure. With the current measurement technique, the position of the IRONSperm had to be selected for 2 frames per measurement only. To determine a more accurate velocity the number of frames to be analyzed would drastically increase so that the path could be reconstructed. Due to time constraints this was not done.

However in future research, it might be very useful to study the velocities more closely. If an accurate image tracking of the IRONSperm is made possible, the time it takes to extract data from the measurement will drastically decrease. Therefore, research into coding that is able to track the IRONSperm in the videos is very useful. To create such software, it is important that the videos are of high enough quality, most importantly, the contrast of IRONSperm and the background should be as high as possible.

7.7.4 Fluid motion

As explained in sec 5.6 the fluid is moving. This has also become evident from the results. Especially figure 15 shows that the measurements are heavily influenced by moving fluid. One easy way in which this response could be improved, is by only measuring the direction that the sperm cell travels in the direction that is oriented in, so in line with the centerline of the flagellum. However, this method assumes that IRONSperm will always moves in a straight line. From experiments, it has been shown that this is mostly true for IRONSperm, and therefore this method would in this case improve the result.

The initial idea to compensate for fluid motion with reference particles was not suitable to use. The reference particles moved in a random motion due to Brownian motion and although the distance they would travel could be estimated with equation 30, estimating the size and shape of the particle is very difficult. Therefore, theoretically the fluid motion that is not caused by Brownian motion can be determined by calculating the distance that a particle will travel as result of Brownian motion and subtracting that from the distance that it has actually travelled. The resultant motion of the particle will then be due to other kind of fluid flows that will also influence the IRONSperm. To accurately apply this approach, accurate measurements are necessary and the dimensions of the particles should be known. In this research the reference particles were of unknown size and therefore there were too many uncertainties to accurately estimate the amount of Brownian motion.

Compensating for Brownian motion could also be done by using glass beads. These are larger than the observed particles and therefore will be less susceptible to the Brownian movement as can be concluded from 32. However, since they are larger, they will also be not as susceptible to fluid motion. Therefore, they will also not be very good to estimate the fluid flow. Still, using these beads can be beneficial, especially if it is possible to make them very small. In that case they can be used to compensate for Brownian motion by using the method described above.

8 Conclusion

The findings of this report can be used to draw conclusions that are useful for further studies. This research shows that the method of the hanging droplet is not preferable for studying IRONSperm. Although the problem of cells sticking to the bottom still remains, it cannot be solved by using the droplet technique. The problem of cells sticking to the bottom, although unfortunate, is not very problematic because there were still enough actuatable free swimming IRONSperm.

Despite trying to achieve multi-flagellar IRONSperm by selecting the samples with high swim-up time and fabricating IRONSperm with spinell particles, no multi-flagellar IRONSperm has been found. Still, IRONSperm with multiple flagella remain of great interest because they will likely swim much faster, which is a useful property in applications. However, the samples that were studied in this research for purpose of multi-flagellar IRONSperm did not produce multi-flagellar IRONSperm. In addition, they were less useful for studying single-flagellar IRONSperm. More research should be conducted to hopefully find multi-flagellar IRONSperm in the future.

It is important to notice that IRONSperm become unsteerable at frequencies above the step-out frequency. Increasing the frequency above the step-out frequency results in an unpredictable swimming direction of the samples. Therefore it is very important that in applications, the step-out frequency of the IRONSperm gets characterized before clinically applying them. Actuating the samples above their step-out frequency should be prevented because there they can not be steered as well as below the step-out frequency.

From the obtained data it can be concluded that these IRONSperm samples are rigid which was unexpected. Due to the rigidness of the flagellum, there is no travelling wave in the flagellum. Still, the flagellum generates thrust in the same way as a flexible flagellum which is described by the resistive force theory.

The observed samples have relatively low swimming speeds and low step-out frequencies. This is likely due to the fact that they have small magnetic moments. More research should be done to prove this hypothesis, but especially due to the low stepout-frequencies, it is very likely that the magnetic moment is very low.

Fluid effects disturbed the measurements more than expected. Therefore, there is a relatively high degree of uncertainty in the measurements of velocity. In future research it is important to take the effects of fluid flow into account so that the results become more accurate. Measures should be taken to eliminate the Brownian noise from the samples, by for instance using glass beads that are larger in diameter and therefore will experience less Brownian motion as reference, or by compensating for Brownian motion with reference particles for which the dimensions are known.

From the obtained results conclusions can be drawn on the effect of field parameters on the swimming speed. It can be seen that there is no clear relationship between the field strength of the external magnetic field and the swimming speed. As long as the frequency is below the step-out frequency, which was the case for the experiment, increasing the field strength does not have an effect. Therefore, in applications, there is not necessarily a need for a high field strength, if the actuation frequency is low.

The frequency response of the sample showed dependency of the swimming speed on the frequency of the external magnetic field. As expected, increasing the frequency results in an increased speed. Once the step-out frequency was reached, there was a clear drop in swimming speed. This shows once again, that it is important that in applications, the IRONSperm are actuated below their step-out frequency.

By combining all found results, the research question can be answered. When exposed to an external rotating magnetic field, IRONSperm that is fabricated from electrostatic self-assembly of sperm cells and rice-grain-shaped maghemite particles, behaves as a rigid swimmer that rotates with the field. The magnetic torque causes IRONSperm to rotate along its long axis which in accordance with the resistive force theory generates a propulsive thrust. This thrust is generated perpendicular to the axis around which the external magnetic field is rotating. IRONSperm therefore swims perpendicular to the external rotating magnetic field. Increasing the frequency of the magnetic field, increases the swimming speed of IRONSperm up to the step-out frequency. Above the step-out frequency the swimming speed drops as the IRONSperm is no longer able to perform full rotations and therefore generates less thrust, which can be seen from the resistive force theory. As long as the frequency is below the step-out frequency, increasing the field strength has no effect on the swimming speed.

References

1. Nelson BJ, Kaliakatsos IK, and Abbott JJ. Microrobots for Minimally Invasive Medicine. Annual Review of Biomedical Engineering 2010; 12. PMID: 20415589:55–85. DOI: 10.1146/annurev-bioeng-010510-103409. Available from: https://doi.org/10.1146/annurev-bioeng-010510-103409
2. Jang D, Jeong J, Song H, and Chung SK. Targeted drug delivery technology using untethered microrobots: a review. Journal of Micromechanics and Microengineering 2019 Mar; 29:053002. DOI: 10.1088/1361-6439/ab087d
3. Society A. Breast cancer facts figures 2017-2018. 2017. Available from: https://bit.ly/3I9BWWd
4. Liyanage PY, Hettiarachchi SD, Zhou Y, Ouhtit A, Seven ES, Oztan CY, Celik E, and Leblanc RM. Nanoparticle-mediated targeted drug delivery for breast cancer treatment. Biochimica et Biophysica Acta (BBA) - Reviews on Cancer 2019; 1871:419–33. DOI: https://doi.org/10.1016/j.bbcan.2019.04.006
5. Magdanz V, Khalil ISM, Simmchen J, Furtado GP, Mohanty S, Gebauer J, Xu H, Klingner A, Aziz A, Medina-Sánchez M, Schmidt OG, and Misra S. IRONSperm: Sperm-templated soft magnetic microrobots. Science Advances 2020; 6:eaba5855. DOI: 10.1126/sciadv.aba5855
6. Magdanz V, Gebauer J, Sharan P, Eltoukhy S, Voigt D, and Simmchen J. Sperm–Particle Interactions and Their Prospects for Charge Mapping. Advanced Biosystems 2019; 3:1900061. DOI: https://doi.org/10.1002/adbi.201900061. Available from: https://onlinelibrary.wiley.com/doi/abs/10.1002/adbi.201900061
7. S. Vijayasarathy PB. Regional differentiation in bull sperm plasma membranes. Biochemical and Biophysical Research Communications 1982; 108:760–9. DOI: https://doi.org/10.1016/0006-291X(82)90894-4. Available from: https://www.sciencedirect.com/science/article/pii/0006291X829
8. Magdanz V, Vivaldi J, Mohanty S, Klingner A, Vendittelli M, Simmchen J, Misra S, and Khalil I. Impact of Segmented Magnetization on the Flagellar Propulsion of Sperm-Templated Microrobots. Advanced Science 2021 Apr; 8. DOI: 10.1002/advs.202004037
9. Khalil ISM, Magdanz V, Simmchen J, Klingner A, and Misra S. Resemblance between motile and magnetically actuated sperm cells. Applied Physics Letters 2020; 116:063702. DOI: 10.1063/1.5142470. Available from: https://doi.org/10.1063/1.5142470
10. MACHIN KE. Wave Propagation along Flagella. Journal of Experimental Biology 1958 Dec; 35:796–806. DOI: 10.1242/jeb.35.4.796. eprint: https://journals.biologists.com/jeb/article-pdf/35/4/796/1337453/796.pdf
11. S. M. Khalil I, Klingner A, and Misra S. Mathematical Modeling of Swimming Soft Microrobots. English. First. Academic Press, 2021 Jun
12. Londhe N, Majumdar R, Rathore J, and Sharma N. SIMULATION OF PLANAR WAVE FLAGELLAR PROPULSION OF NANOROBOTS USING COMSOL. 2011 Nov
13. Friedrich B, Riedel-Kruse I, Howard J, and Jülicher F. High-precision tracking of sperm swimming fine structure provides strong test of resistive force theory. The Journal of experimental biology 2010 Apr; 213:1226–34. DOI: 10.1242/jeb.039800
14. Gars YJL. Influence of bovine spermataozoa bundling on flagellar wave propagation
15. Woolley D and Vernon G. A study of helical and planar waves on sea urchin sperm flagella, with a theory of how they are generated. Journal of Experimental Biology 2001 Apr; 204:1333–45. DOI: 10.1242/jeb.204.7.1333. eprint: https://journals.biologists.com/jeb/article-pdf/204/7/1333/1239643/1333.pdf
16. Khalil ISM, Tabak AF, Abou Seif M, Klingner A, and Sitti M. Controllable switching between planar and helical flagellar swimming of a soft robotic sperm. PLOS ONE 2018 Nov; 13:1–15. DOI: 10.1371/journal.pone.0206456. Available from: https://doi.org/10.1371/journal.pone.0%2006456
17. Xu T, Yu J, Yan X, Choi H, and Zhang L. Magnetic Actuation Based Motion Control for Microrobots: An Overview. Micromachines 2015; 6:1346–64. DOI: 10.3390/mi6091346. Available from: https://www.mdpi.com/2072-666X/6/9/1346
18. Peyer KE, Mahoney AW, Zhang L, Abbott JJ, and Nelson BJ. Chapter 7 - Bacteria-Inspired Microrobots. Ed. by Kim M, Julius AA, and Steager E. Micro and Nano Technologies. Boston: William Andrew Publishing, 2012 :165–99. DOI: https://doi.org/10.1016/B978-1-4557-7891-1.00007-4. Available from: https://www.sciencedirect.com/science/article/pii/B9781455778911000074
19. Caldag HO and Yesilyurt S. Acoustic radiation forces on magnetically actuated helical swimmers. Physics of Fluids 2020; 32:092012. DOI: 10.1063/5.0020930. Available from: https://doi.org/10.1063/5.0020930
20. Hosney A, Klingner A, Misra S, and Khalil ISM. Propulsion and steering of helical magnetic microrobots using two synchronized rotating dipole fields in three-dimensional space. 2015 :1988–93. DOI: 10.1109/IROS.2015.7353639

21. Temel FZ, Bezer AE, and Yesilyurt S. Navigation of mini swimmers in channel networks with magnetic fields. 2013 :5335–40. DOI: 10.1109/ICRA.2013.6631341

22. Temel FZ and Yesilyurt S. Magnetically actuated micro swimming of bio-inspired robots in mini channels. 2011 :342–7. DOI: 10.1109/ICMECH.2011.5971307

23. Xu T, Yu J, Vong CI, Wang B, Wu X, and Zhang L. Dynamic Morphology and Swimming Properties of Rotating Miniature Swimmers With Soft Tails. IEEE/ASME Transactions on Mechatronics 2019; 24:924–34. DOI: 10.1109/TMECH.2019.2912404

24. Abbott JJ, Peyer KE, Lagomarsino MC, Zhang L, Dong L, Kaliakatsos IK, and Nelson BJ. How Should Microrobots Swim? The International Journal of Robotics Research 2009; 28:1434–47. DOI: 10.1177/0278364909341658

25. Peyer KE, Qiu F, Zhang L, and Nelson BJ. Movement of artificial bacterial flagella in heterogeneous viscous environments at the microscale. 2012 :2553–8. DOI: 10.1109/IROS.2012.6386096

26. Mahoney AW, Nelson ND, Peyer KE, Nelson BJ, and Abbott JJ. Behavior of rotating magnetic microrobots above the step-out frequency with application to control of multi-microrobot systems. Applied Physics Letters 2014; 104:144101. DOI: 10.1063/1.4870768

27. O'Brien J. A Mathematical Model of Fluid Flow in Evaporating Droplets Using Wedge Geometry. Rochester Institute of Technology 2018. Available from: https://scholarworks.rit.edu/cgi/viewcontent.cgi?article=11051&context=theses

28. Abbott J, Ergeneman O, Kummer M, Hirt A, and Nelson B. Modeling Magnetic Torque and Force for Controlled Manipulation of Soft-Magnetic Bodies. IEEE Transactions on Robotics 2007 Dec; 23:1247–52. DOI: 10.1109/TRO.2007.910775

A Appendix A: Drag anisotropy

As seen in equation 13 an inequality in drag forces has to occur to ensure propulsion. Drag anisotropy is a result of having a long slender element, such as a flagellum. The slenderness results in the fact that it is harder to move in the direction normal to the element.

The drag ansisotropy can also be found as a result of the flow at low Reynolds numbers. The dynamics of fluids can be described by the Navier-Stokes equations.

$$\rho(\frac{\partial}{\partial \mathrm{t}} + \mathrm{u} * \nabla)\mathrm{u} = \nabla \mathrm{p} + \eta \nabla^2 \mathrm{u} \tag{A.1}$$

$$\nabla * \mathrm{u} = 0 \tag{A.2}$$

In these equations, ρ is the density, η is the viscous force and u is the velocity field of the fluid. At very low Reynolds numbers, which is applicable for this system, inertial forces are negligible and it can be assumed that the flow stops immediately when the force stops.
The Navier Stokes equations are linear so it is allowed to use mathematical methods that rely on superposition to solve for the pressure and flow fields [1]. One possible solution is found using Green functions [2]

$$\overrightarrow{f}^{ext} = \overrightarrow{F}\delta(\overrightarrow{r}) \tag{A.3}$$

This solution is known as a stokeslet. F is a constant force vector and $\delta(r)$ is the three-dimensional Dirac delta.The stokeslet physically represents the flow field due to a point force F acting on the fluid at the origin of the coordinate system. The velocity and pressure of a Stokeslet are respectively:

$$\overrightarrow{u} = \frac{1}{8\pi\eta}(\frac{\overrightarrow{F}}{r} + \frac{(\overrightarrow{r} * \overrightarrow{F}) * \overrightarrow{r}}{r^3}) \tag{A.4}$$

$$p = \frac{\overrightarrow{r} * \overrightarrow{F}}{4\pi r^3} \tag{A.5}$$

From these equations, it can be seen that the velocity decays in space as 1/r and the pressure field decays in space as $1/r^2$. Where r is the distance from the origin.

Evaluating equation A.4 in the direction parallel and perpendicular to the applied force yields:

$$u_{\parallel} = (\overrightarrow{u} * \frac{\overrightarrow{F}}{F})_{\overrightarrow{r} * \overrightarrow{F} = rF} = \frac{F}{4\pi r\eta} \tag{A.6}$$

$$u_{\perp} = (\overrightarrow{u} * \frac{\overrightarrow{F}}{F})_{\overrightarrow{r} * \overrightarrow{F} = 0} = \frac{F}{8\pi r\eta} \tag{A.7}$$

These equations show that the velocity in the parallel direction is twice as great as that in normal direction. So, to obtain the same velocity the force in perpendicular direction has to be twice as large. This shows the anisotropy necessary for the drag based thrust [1,2].

The above derivation is assuming an infinitely slender element. For IRONSperm, it is appropriate to use the values expressed in equation B.15 and B.14 so:

$$\xi_{\parallel} = \frac{2\pi\eta}{\ln(L/r) - 0.807} \tag{A.8}$$

$$\xi_{\perp} = \frac{2\pi\eta}{\ln(L/r) + 0.193} \tag{A.9}$$

These exact values are dependent on the viscosity of the fluid and the ratio between the flagellar length and radius. From these values, it still follows that there is a drag anisotropy and therefore a propulsive force.

B Appendix B: Drag matrix coefficients

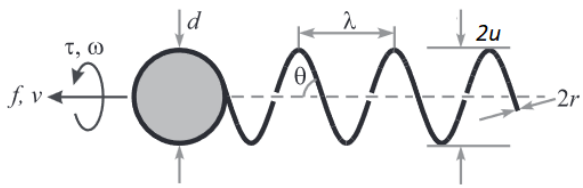

Figure B.1: The values that are used to determine the drag coefficients.[3]

The actuation of the IRONSperm can be described by the following equation:

$$\begin{bmatrix} \overrightarrow{F_m} \\ \overrightarrow{T_m} \end{bmatrix} = \begin{bmatrix} \mathrm{a} & \mathrm{b} \\ \mathrm{b} & \mathrm{c} \end{bmatrix} \begin{bmatrix} \overrightarrow{v} \\ \overrightarrow{\omega} \end{bmatrix} \tag{B.10}$$

Here F_m and T_m are defined the magnetic force and magnetic torque. V is the linear velocity and ω is the rotational velocity. The coefficients of the drag matrix are experimentally determined for the case where a flagellum is rigidly attached to a body [3]. They depend on the viscosity of the fluid and the geometrical properties of the swimmer [3,4].

$$\mathrm{a} = 2\pi \mathrm{nr} \frac{\xi_{\parallel} \cos^2(\theta) + \xi_{\perp} \sin^2(\theta)}{\sin(\theta)} \tag{B.11}$$

$$\mathrm{b} = 2\pi \mathrm{nr}^2 (\xi_{\parallel} - \xi_{\perp}) \cos(\theta) \tag{B.12}$$

$$\mathrm{c} = 2\pi \mathrm{nr}^3 \frac{\xi_{\perp} \cos^2 + \xi_{\parallel} \sin^2 \theta}{\sin \theta} \tag{B.13}$$

The parameters are defined according to figure B.1. n is the number of turns of the helix, u is the amplitude of the wave as seen from the center line, θ is the angle between the tail and the central line. $\xi_{\parallel}$ and $\xi_{\perp}$ are the viscous drag coefficients and can be expressed as [5]:

$$\xi_{\parallel} = \frac{2\pi\eta}{\ln(\mathrm{L/r}) - 0.807} \tag{B.14}$$

$$\xi_{\perp} = \frac{2\pi\eta}{\ln(\mathrm{L/r}) + 0.193} \tag{B.15}$$

To compensate for the attached head, the drag coefficients of the head should be added to the linear matrix from equation B.16. Therefore the new equation becomes:

$$\begin{bmatrix} \overrightarrow{F_m} \\ \overrightarrow{T_m} \end{bmatrix} = \begin{bmatrix} \mathrm{a} + \psi_{\mathrm{v}} & \mathrm{b} \\ \mathrm{b} & \mathrm{c} + \psi_{\omega} \end{bmatrix} \begin{bmatrix} \overrightarrow{v} \\ \overrightarrow{\omega} \end{bmatrix} \tag{B.16}$$

Here ψ_v and ψ_ω are the translational and rotational drag coefficients for the head. They are defined as follows assuming the head is circular:

$$\psi_{\mathrm{v}} = \pi\eta \mathrm{d}^3 \tag{B.17}$$

$$\psi_{\omega} = \pi\eta \mathrm{d}^3 \tag{B.18}$$

B.1 Estimation of the magnetic moment

To estimate the magnetic moment of the sample, the relation between the step-out frequency and the maximum torque can be used. The equation is derived in 4.3.3 and is:

$$\mathrm{f_{SO}} = \frac{1}{2\pi} \frac{\mathrm{a} + \psi_{\mathrm{v}}}{(\mathrm{a} + \psi_{\mathrm{v}})(\mathrm{c} + \psi_{\omega}) - \mathrm{b}^2} \mathrm{T_{max}} \tag{B.19}$$

The magnetic moment of the used samples is unknown, but estimates of the magnetic moment of similarly fabricated IRONSperm are known from previous research.

The magnetic moment has been estimated for IRONSperm from which the frequency response can be found in 17. This IRONSperm can be seen in figure B.2.

Figure B.2: The IRONSperm for which the magnetic moment is estimated by estimating the coefficients of the drag matrix.

The parameters have been measured and estimated as follows:

$$\begin{aligned} \mathrm{n} &= 2 \\ \mathrm{r} &= 3 \times 10^{-6} \\ \eta &= 0.7 \\ \mathrm{d} &= 0.4 * 1.14 \times 10^{-5} \\ \theta &= 37 \\ \mathrm{L} &= 3* \\ \mathrm{B} &= 5 \times 10^{-3} \\ \mathrm{f_{so}} &= 0.8 \end{aligned}$$

Using this values a magnetic moment of 1.3100×10^{-12} Am^2 was found for a field strength of 5 mT. Earlier research found the magnetic moment of IRONSperm to be 5.9×10^{-11} Am^2. The samples in that research also show a much higher step-out frequency. It can thus be said that the magnetic moment of the samples that were used in this research were relatively low.

However, the method used to determine the magnetic moment is too inaccurate. The parameters from which the drag matrix is built up can not be estimated exact enough. The model is defined for a perfectly helical shape and figure B.2 shows that the flagellar wave is clearly not a perfect helix. Therefore, it has been chosen to no include these results in the main part of the report. However, if the parameters of the drag matrix can be more accurately determined, this method could be useful to estimate the magnetic moment of the samples. Conversely, in case the magnetic moment of the samples is known, formula B.19 can be used to predict the step-out frequencies.

References of the appendix

[1] Lauga E and Powers TR. The hydrodynamics of swimming microorganisms. Reports on Progress in Physics 2009 Aug; 72:096601. doi: 10.1088/0034-4885/72/9/096601. Available from: https://doi.org/10.1088/0034-4885/72/9/09

[2] Dennis Brojan RP. Life at low Reynolds numbers. 2009 May. Available from: http://www- f1.ijs.si/ rudi/sola/seminar-brojan.pdf

[3] Abbott JJ, Peyer KE, Lagomarsino MC, Zhang L, Dong L, Kaliakatsos IK, and Nelson BJ. How Should Microrobots Swim? The International Journal of Robotics Research 2009; 28:1434–47. doi: 10.1177/027836490934165

[4] Xu T, Yu J, Vong CI, Wang B, Wu X, and Zhang L. Dynamic Morphology and Swimming Properties of Rotating Miniature Swimmers With Soft Tails. IEEE/ASME Transactions on Mechatronics 2019; 24:924–34. doi: 10.1109/TMECH.2019.2912

[5] Magdanz V, Vivaldi J, Mohanty S, Klingner A, Vendittelli M, Simmchen J, Misra S, and Khalil I. Impact of Segmented Magnetization on the Flagellar Propulsion of Sperm-Templated Microrobots. Advanced Sci- ence 2021 Apr; 8. doi: 10.1002/advs.202004